Angewandte Chemie
Eine Zeitschrift der Gesellschaft Deutscher Chemiker

Supporting Information

Insertion of CO_2 Mediated by a (Xantphos)Ni^I–Alkyl Species

*Justin B. Diccianni, Chunhua T. Hu, and Tianning Diao**

anie_201906005_sm_miscellaneous_information.pdf

Supporting Information

Table of Contents

1. Experimental Details

General Considerations

All air- and moisture- sensitive manipulations were carried out in a nitrogen-filled glove box. Volatiles and liquid chemicals were dried over CaH_2 and distilled prior to use. Solvents were dried and deoxygenated by passing through alumina in a solvent purification system. *t*-BuXantphos was purchased from commercial sources and used without further purification. $NiBr_2$(DME) was synthesized according to a literature procedure.[1] Chloroform-*d* was purchased from Cambridge Isotope Laboratories and used as received. Benzene-d_6 was purchased from Cambridge Isotope Laboratories, dried over 4 Å mol. sieves for one month, degassed, and stored in a nitrogen-filled glove box over 4 Å mol. sieves. Carbon dioxide was purchased from Airgas and was passed through two Drierite columns before use.

^{1}H, ^{31}P, and ^{13}C NMR spectra were recorded on Bruker 600,[2] 500, and 400 MHz Avance spectrometers. The chemical shifts (δ) are given in parts per million and referenced to residual solvent peaks. The following abbreviations were used to describe multiplicities: s = singlet, d = doublet, t = triplet, q = quartet, sept = septet, m = multiplet, br = broad, v br = very broad. High resolution mass spectra (HRMS) were collected on an Agilent 6224 TOF LC/MS. Organic reactions were monitored by thin-layer chromatography (TLC) on Merck TLC silica gel 60 F254 plates and compounds were visualized by UV light (254 nm) or KMnO4 staining. Column chromatography was performed on Merck silica gel 60 (0.015−0.040 mm). IR spectra were recorded on a Nicolet 6700 FT-IR spectrometer in KBr pellets. UV-vis spectra were recorded on a Cary 100 Bio UV-Visible spectrophotometer. All single crystal data were collected on a Bruker SMART APEXII CCD Diffractometer equipped with an Oxford Cryosystems 700+ Cooler. Continuous wave (CW) EPR spectra were recorded on a Bruker X-band EMXPlus spectrometer equipped with an EMX standard resonator and a Bruker PremiumX microwave bridge. The spectra were simulated using EasySpin[3] for MATLAB.

Experimental Procedures and Characterization

(*t*-BuXantphos)$NiBr_2$ (1)

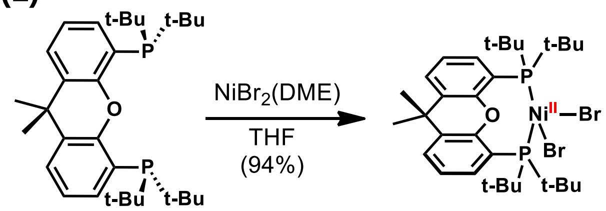

A 20 mL scintillation vial was charged with 437 mg *t*-BuXantphos (0.88 mmol, 1 equiv) and 270 mg $NiBr_2$(DME) (0.88 mmol, 1 equiv). THF (10 mL) was added to the vial and the mixture was stirred at r.t. overnight. The mixture was filtered through a pad of celite and solvent was removed from the filtrate. The product was obtained as a brown powder (593 mg, 0.83 mmol 94%). Crystals suitable for XRD were grown by layering a THF solution of **1** with Et_2O and allowing the solvents to diffuse at r.t. for several days.

^{1}H NMR (400 MHz, C6D6, 25 °C, δ): 25.92 (br s, 2H), 24.98 (s, 2H), 17.23 (s, 2H), 13.90 (v br s, 36H), -2.34 (s, 6H). This compound shows no ^{13}C or ^{31}P NMR spectra.

UV-Vis (THF, 23 °C): 285 nm (ε = 8.39 × 10^3 $M^{-1}cm^{-1}$); 385 nm (ε = 2.94 × 10^3 $M^{-1}cm^{-1}$).

(*t*-BuXantphos)NiBr·$ZnBr_2$(THF) + (*t*-BuXantphos)NiBr (2)

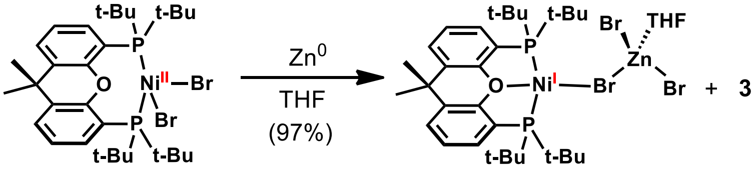

A 20 mL scintillation vial was charged with (*t*-BuXantphos)$NiBr_2$ (33 mg, 0.046 mmol, 1 equiv) and 5 mL THF. Zn powder (15 mg, 0.23 mmol, 3 equiv) was added and the mixture was stirred at room temperature. The solution color changed from brown to green to yellow. Stirring was continued for two hours, then the mixture was filtered to remove excess Zn. The yellow THF solution was layered with pentane and stored at –35 °C. Yellow plate-like crystals of **2** formed over five days (35.2 mg, 0.022 mmol, 97%).

^{1}H NMR (400 MHz, C_6D_6, 25 °C, δ): 15.28 (v br s, 4H), 13.13 (br s, 4H), 9.93 (v br s, 4H), 3.86 (v br s, 72H), 3.39 (br s, 4H), 1.36 (br s, 4H), -0.63 (br s, 12H). This compound shows no ^{13}C or ^{31}P NMR spectra. Despite the crystal structure indicating one molecule of **3** is present, the chemical shifts of **3** are absent in the NMR and only one species is observed. This may be due to a bridged dimer that forms in solution.

UV-Vis (THF, 23 °C): 275 nm (ε = 4.79 × 10^3 $M^{-1}cm^{-1}$); 395 nm (ε = 1.32 × 10^3 $M^{-1}cm^{-1}$).

(*t*-BuXantphos)NiBr (3)

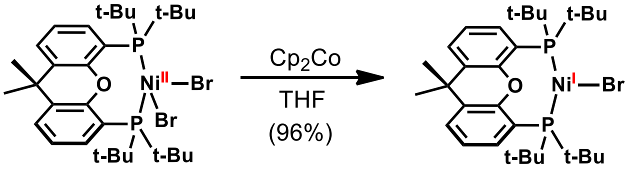

A 20 mL scintillation vial was charged with 330 mg **1** (0.46 mmol, 1 equiv) and 10 mL THF. Separately, 87 mg Cp_2Co (0.46 mmol, 1 equiv) was dissolved in 4 mL THF. The Cp_2Co solution was added to the solution of **1** and the reaction turned yellow, concomitant with the precipitation of a yellow/green solid. The mixture was allowed to stir at r.t. for 1.5 hrs, then filtered through a pad of celite. Solvent was removed from the filtrate to give a dark yellow powder. The residue was dissolved in 5 mL THF and 1 mL toluene, filtered, then layered with pentane and stored at –35 °C. The product was obtained as canary yellow needle-like crystals (280 mg, 0.44 mmol, 96%).

^{1}H NMR (400 MHz, C6D6, 25 °C, δ): 16.61 (br s, 2H), 12.87 (s, 2H), 11.05 (br s, 2H), 3.71 (v br s, 36H), -0.56 (s, 6H). This compound shows no ^{13}C or ^{31}P NMR spectra.
UV-Vis (THF, 23 °C): 230 nm (shoulder); 275 nm ($\varepsilon = 1.78 \times 10^3$ $M^{-1}cm^{-1}$); 310 nm ($\varepsilon = 8.92 \times 10^2$ $M^{-1}cm^{-1}$); 410 nm ($\varepsilon = 4.63 \times 10^2$ $M^{-1}cm^{-1}$).
Anal. Calcd. for $C_{31}H_{48}BrNiOP_2$: C, 58.43; H, 7.59. **Found:** C, 58.77; H, 7.54.

(*t*-BuXantphos)Ni(I)Me (4)

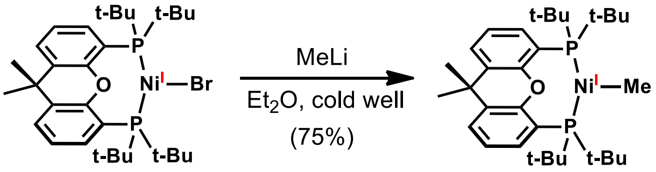

A 20 mL scintillation vial was charged with (*t*-BuXantphos)NiBr (36 mg, 0.056 mmol, 1 equiv) and 5 mL Et$_2$O. The mixture was cooled in a liquid N$_2$-filled cold well. MeLi (42 µL of 1.6 M solution, 0.068 mmol, 1.2 equiv) was added and the solution turned brown. The mixture was intermittently stirred at room temperature for 15 second intervals and cooled down in the cold well in between stirring to ensure the temperature remained low. Once the mixture had become homogeneous (all (*t*-BuXantphos)NiBr dissolved), it was left in the cold well for 1 hour to react. Solvent was removed in the cold well. The brown residue was extracted with cold pentane and filtered through a pre-cooled glass filter in a pipette. Pentane was removed to give a brown solid (24 mg, 0.042 mmol, 75%). Crystals suitable for XRD were grown by allowing a concentrated pentane solution of (*t*-BuXantphos)Ni(I)Me to slowly evaporate at –35 °C for several days. Satisfactory elemental analysis could not be obtained for this compound due to extreme air and thermal sensitivity.
^{1}H NMR (500 MHz, C_6D_6, 25 °C, δ): 25.22 (br s, 2H), 18.40 (br s, 2H), 9.12 (s, 2H), 2.96 (v br s, 36H), 0.26 (s, 6H). The resonance for the Me group is not observe due to paramagnetic broadening. This compound shows no ^{13}C or ^{31}P NMR spectra.
UV-Vis (pentane, 0 °C): 365 nm ($\varepsilon = 1.37 \times 10^3$ $M^{-1}cm^{-1}$); 415 nm ($\varepsilon = 1.05 \times 10^3$ $M^{-1}cm^{-1}$).

(*t*-BuXantphos)Ni(I)Et (5)

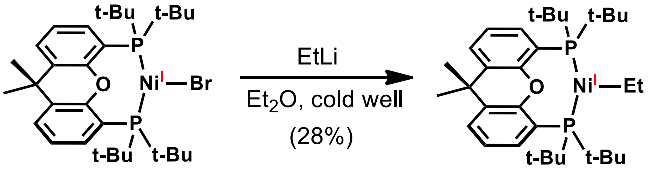

A 20 mL scintillation vial was charged with (*t*-BuXantphos)NiBr (36 mg, 0.056 mmol, 1 equiv) and 5 mL Et$_2$O. The mixture was cooled in a liquid N$_2$-filled cold well. EtLi (136 µL of 0.5 M solution, 0.068 mmol, 1.2 equiv) was added and the solution turned brown. The mixture was intermittently stirred at room temperature for 15 second intervals and cooled down in the cold well in between stirring to ensure the temperature remained low. Once the mixture had become homogeneous (all (*t*-BuXantphos)NiBr dissolved), it was left in the cold well for 1 hour to react. Solvent was removed in the cold well. The brown residue was extracted with cold pentane and filtered through a pre-cooled glass filter in a pipette. Pentane was removed to give a brown oil. The oil was dissolved in 0.6 mL C_6D_6, 1 mesitylene was added, and the mixture was analyzed by ^1H NMR (28% yield). The compound is very sensitive and decomposes rapidly, with release of ethylene, at room temperature. Crystals suitable for XRD were grown by allowing a concentrated pentane solution of (*t*-BuXantphos)Ni(I)Et to slowly evaporate at –35 °C for several days. Satisfactory elemental analysis could not be obtained for this compound due to extreme air and thermal sensitivity.

^{1}H NMR (500 MHz, C_6D_6, 25 °C, δ): 23.28 (br s, 2H), 17.72 (s, 2H), 8.16 (br s, 2H), 3.45 (v br s, 36H), -0.36 (s, 6H). The resonances for the Et group are not observed due to paramagnetic broadening. This compound shows no ^{13}C or ^{31}P NMR spectra.

UV-Vis (pentane, 23 °C): 370 nm ($\varepsilon = 1.02 \times 10^3\ M^{-1}cm^{-1}$); 420 nm ($\varepsilon = 9.1 \times 10^2\ M^{-1}cm^{-1}$).

(*t*-BuXantphos)Ni(I)OAc (9)

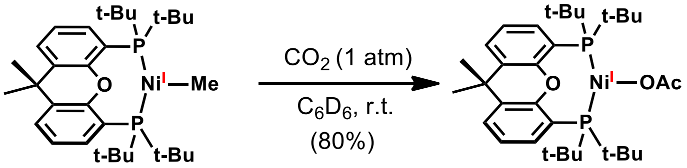

A J-Young NMR tube was charged with (*t*-BuXantphos)Ni(I)Me (20 mg, 0.034 mmol, 1 equiv) in 0.6 mL C_6D_6. The solution was frozen, degassed, and refilled with 1 atm CO_2. Upon thawing, the brown solution quickly turned orange. Volatiles were removed from the orange solution, the residue was extracted with pentane, and the pentane solution was filtered and stored at –35 °C to crystallize. Orange, needle-like crystals of (*t*-BuXantphos)Ni(I)OAc formed overnight (17 mg, 0.028 mmol, 80%). Satisfactory elemental analysis could not be obtained for this compound due to air and thermal sensitivity.

^{1}H NMR (500 MHz, C_6D_6, 25 °C, δ): 16.64 (br s, 2H), 12.76 (s, 2H), 12.43 (br s, 2H), 8.60 (br s, 3H), 3.68 (v br s, 36H), -0.94 (s, 6H).This compound shows no ^{13}C or ^{31}P NMR spectra.

UV-Vis (THF, 23 °C): 465 nm ($\varepsilon = 5.83 \times 10^3\ M^{-1}cm^{-1}$).

(*t*-BuXantphos)Ni(I)CO_2Et (10)

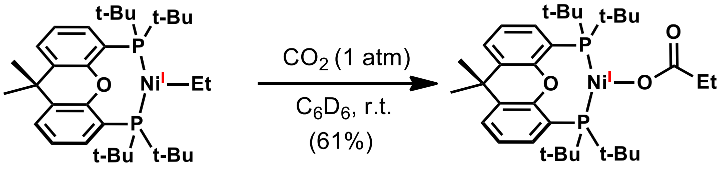

A J-Young NMR tube was charged with (*t*-BuXantphos)Ni(I)Et (0.016 mmol, 1 equiv) in 0.6 mL C_6D_6. The solution was frozen, degassed, and refilled with 1 atm CO_2.

Upon thawing, the brown solution quickly turned orange. Volatiles were removed from the orange solution, the residue was extracted with pentane, and the pentane solution was filtered and stored at –35 °C to crystallize. Orange, needle-like crystals of (*t*-BuXantphos)Ni(I)CO_2Et formed overnight (6 mg, 0.01 mmol, 61%). Satisfactory elemental analysis could not be obtained for this compound due to air and thermal sensitivity.

^{1}H NMR (500 MHz, C_6D_6, 25 °C, δ): 16.67 (br s, 2H), 12.75 (s, 2H), 12.45 (br s, 2H), 3.67 (v br s, 36H), 2.34 (br s, 2H), 0.43 (br s, 3H), -0.95 (s, 6H). This compound shows no ^{13}C or ^{31}P NMR spectra.

UV-Vis (THF, 23 °C): 470 nm ($\varepsilon = 6.21 \times 10^3$ $M^{-1}cm^{-1}$).

(*t*-BuXantphos)Ni(I)Ph (11)

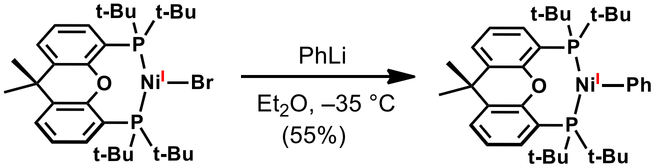

A 20 mL scintillation vial was charged with (*t*-BuXantphos)NiBr (70 mg, 0.11 mmol, 1 equiv) and 10 mL Et_2O to form a slurry. The mixture was cooled to –35 °C. A solution of PhLi in Et_2O (0.13 mmol, 1.2 equiv) was added to the cold slurry of (*t*-BuXantphos)NiBr. The color changed from yellow to brown and the mixture was stirred at r.t. for one hour. Solvent was removed from the brown solution. Purification was accomplished by extraction with pentane followed by crystallization from pentane at –35 °C to yield the product as dark brown blocks (37 mg, 0.058 mmol, 55%).

^{1}H NMR (400 MHz, C_6D_6, 25 °C, δ): 41.61 (v br s, 2H), 23.98 (br s, 2H), 22.84 (br s, 1H), 18.04 (br s, 2H), 9.37 (s, 2H), 2.68 (v br s, 36H), 0.50 (s, 6H). The resonances for the *ortho* protons on the phenyl ring are not observed due to paramagnetic broadening. This compound shows no ^{13}C or ^{31}P NMR spectra.

UV-Vis (pentane, 23 °C): 250 nm ($\varepsilon = 5.48 \times 10^3$ $M^{-1}cm^{-1}$); 290 nm ($\varepsilon = 3.18 \times 10^3$ $M^{-1}cm^{-1}$).

Anal. Calcd. for $C_{37}H_{53}NiOP_2$: C, 70.04; H, 8.42. **Found:** C, 70.34; H, 8.44.

HRMS (ESI-TOF) m/z: [M + H]+ calcd for $C_{37}H_{54}NiOP_2$ 634.3003, found 634.3082.

(*t*-BuXantphos)Ni(I)-phenylacetylide (7)

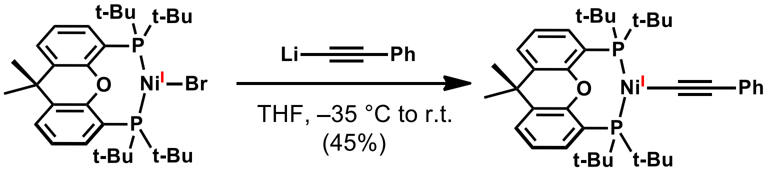

A 20 mL scintillation vial was charged with (*t*-BuXantphos)NiBr (15 mg, 0.024 mmol, 1 equiv) and 2 mL THF. The solution was cooled to –35 °C. Lithium phenylacetylide (3.9 mg, 0.036 mmol, 1.5 equiv) was added in 0.5 mL THF and the solution was stirred at room temperature for 10 minutes. Solvent was removed from the brown solution and the residue was extracted with pentane, filtered, and stored at –35 °C. The product precipitated as a red/brown powder (7.1 mg, 0.011 mmol, 45%). This compound decomposes at room temperature. Satisfactory elemental analysis could not be obtained for this compound due to air and thermal sensitivity.

^{1}H NMR (400 MHz, C_6D_6, 25 °C, δ): 25.01 (v br s, 2H), 16.91 (br s, 2H), 12.22 (br s, 1H), 10.75 (br s, 2H), 10.36 (br s, 1H), 5.56 (br s, 2H), 2.67 (v br s, 36H), 0.40 (br s, 6H). This compound shows no ^{13}C or ^{31}P NMR spectra.

UV-Vis (pentane, 23 °C): 290 nm (ε = 1.12×10^2 $M^{-1}cm^{-1}$); 410 nm (ε = 2.93×10^3 $M^{-1}cm^{-1}$).

(*t*-BuXantphos)Ni(I)-acetylide (6)

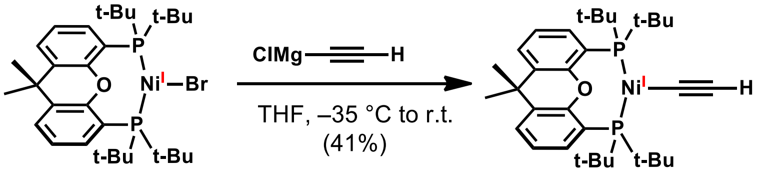

A 20 mL scintillation vial was charged with (*t*-BuXantphos)NiBr (15 mg, 0.024 mmol, 1 equiv) and 2 mL THF. The solution was cooled to –35 °C. A solution of the Grignard reagent (58 µL of 0.6 M solution, 0.036 mmol, 1.5 equiv) was added and the solution was stirred at room temperature for 30 minutes. Solvent was removed from the orange solution and the residue was extracted with pentane, filtered, and stored at –35 °C. The product crystallized as red/orange blocks (5.8 mg, 0.01 mmol, 41%). This compound decomposes at room temperature over 1-2 days. Satisfactory elemental analysis could not be obtained for this compound due to air and thermal sensitivity.

^{1}H NMR (400 MHz, C_6D_6, 25 °C, δ): 24.90 (v br s, 2H), 17.05 (v br s, 2H), 12.00 (br s, 1H), 2.54 (v br s, 36H), 0.36 (br s, 6H). The resonance for the alkyne proton is not observed due to paramagnetic broadening. This compound shows no ^{13}C or ^{31}P NMR spectra.

UV-Vis (pentane, 23 °C): 330 nm (ε = 8.42×10^3 $M^{-1}cm^{-1}$); 290 nm (ε = 3.18×10^3 $M^{-1}cm^{-1}$).

(*t*-BuXantphos)Ni(I)OPh (8)

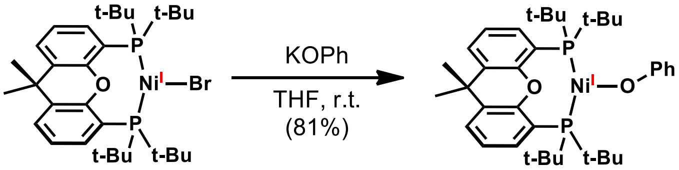

A 20 mL scintillation vial was charged with (*t*-BuXantphos)NiBr (24 mg, 0.038 mmol, 1 equiv), KOPh (7.3 mg, 0.056 mmol, 1.5 equiv), and THF (2mL). The solution was stirred overnight, filtered, and layered with pentane at –35 °C. Small yellow crystals of the product formed over three days (20 mg, 0.031 mmol, 81%). Satisfactory elemental analysis could not be obtained for this compound due to air sensitivity.

^{1}H NMR (400 MHz, C_6D_6, 25 °C, δ): 15.47 (s, 2H), 13.80 (s, 2H), 11.33 (s, 2H), 10.83 (s, 2H), 4.64 (s, 36H), -0.48 (s, 6H), -2.10 (s, 1H). The resonance for the *ortho* protons on

the phenoxide are not observed due to paramagnetic broadening. This compound shows no ^{13}C or ^{31}P NMR spectra.
UV-Vis (THF, 23 °C): 395 nm ($\varepsilon = 3.71 \times 10^3$ $M^{-1}cm^{-1}$).

(Ph-Xantphos)Ni(II)BrPh

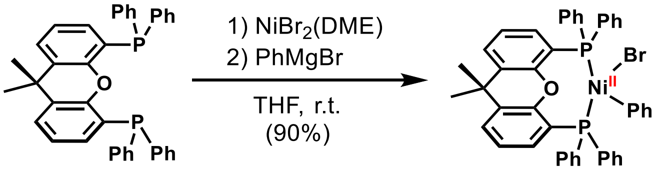

A 20 mL scintillation vial was charged with Ph-Xantphos (416 mg, 0.72 mmol, 1 equiv), $NiBr_2$(DME) (222 mg, 0.72 mmol, 1 equiv), and 10 mL THF. The mixture was stirred for 20 minutes at room temperature, over which time a green precipitate forms. The mixture was cooled to –35 °C, then PhMgBr (0.24 mL, 3 M solution in Et_2O, 0.72 mmol, 1 equiv) was added and the reaction mixture turned red. After stirring at room temperature for 2 hours, the mixture was cooled to –35 °C, then filtered to collect a red solid. The filter cake was washed with cold THF, then Et_2O, and dried under vacuum. The product was collected as a red powder in 90% yield (515 mg, 0.65 mmol).
^{1}H NMR (400 MHz, C_6D_6, 25 °C, δ): 7.39-7.33 (m, 2H), 7.03 (br d, *J* = 6.5 Hz, 2H), 6.97-6.93 (m, 2H), 6.81 (t, *J* = 7.6 Hz, 2H), 6.43 (t, *J* = 7.1 Hz, 1H), 6.33 (t, *J* = 7.6 Hz, 2H), 1.49 (s, 6H). This compound shows no ^{13}C NMR spectrum, consistent with previously reported (Ph-Xantphos)NiArX compounds.[4]
^{31}P NMR (162 MHz, C_6D_6, 25 °C, δ): 8.67.

Carboxylation of *in-situ* Generated (Ph-Xantphos)Ni(I)Ph

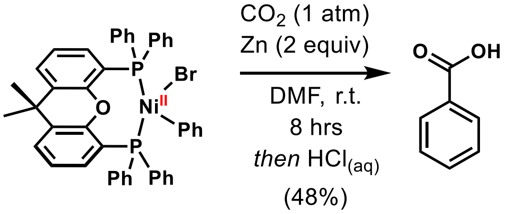

A 4 mL vial with a septum cap was charged with 49 mg (Ph-Xantphos)Ni(II)BrPh (0.06 mmol, 1 equiv), 8 mg Zn (0.12 mmol, 2 equiv), and a stir bar. The vial was capped, removed from the glove box, and purged with CO_2 from a balloon (~0.5 L). DMF (0.5 mL) was added and the red reaction mixture was stirred under CO_2 for 8 hours. The now brown reaction mixture was quenched with 1 M $HCl_{(aq)}$ (2 mL) and extracted with Et_2O (3 x 2 mL). The organic phase was extracted with 1 M $NaOH_{(aq)}$ (4 x 3 mL). The aqueous phase was extracted with Et_2O (2 x 2 mL). The aqueous phase was acidified to pH 1 with 3 M $HCl_{(aq)}$ and extracted with Et_2O (3 x 5 mL). The organic was dried over Na_2SO_4 and solvent was removed. The residue was dissolved in 0.6 mL $CDCl_3$ with 0.5 µL of mesitylene internal standard added for NMR analysis. The yield of benzoic acid was determined to be 48% by ^{1}H NMR.

When run under identical conditions, but without Zn added, no benzoic acid is observed by ^{1}H NMR.

General Procedure for Attempts at Promoting CO_2 Insertion into Ni–X Bonds

A J-Young NMR tube was charged with a Ni compound (1 equiv) and a Lewis acid (1 equiv) in 0.6 mL C_6D_6. The solution was frozen, degassed, and refilled with 1 atm CO_2. The contents were shaken thoroughly to ensure liquid-gas mixing. The products were analyzed by NMR spectroscopy.

2. Catalytic Reactions

Carboxylation of PhZnCl

$$\mathrm{PhZnCl} \xrightarrow[\substack{\text{THF} \\ \text{r.t., 12 hrs.} \\ \textit{then}\ \text{HCl}}]{\substack{CO_2\ \text{(1 atm)} \\ \text{[Ni] (10\%)}}} \mathrm{PhCO_2H}$$

A bomb flask was charged with Ni catalyst (0.018 mmol, 0.1 equiv), evacuated, then refilled with CO_2. Under a stream of CO_2, a solution of PhZnCl (0.18 mmol, 1 equiv) in 2 mL THF was added. The bomb flask was sealed and the reaction mixture was stirred at room temperature for 12 hours. The mixture was quenched with 10% aqueous HCl and extracted with Et_2O three times. The organic phase was extracted with 10% aqueous KOH three times. The aqueous phase was washed with two portions of Et_2O. The aqueous phase was brought to pH 1 by addition of HCl and extracted with Et_2O three times. Solvent was removed and the residue was dissolved in $CDCl_3$ with 0.5 µL of mesitylene internal standard added for NMR analysis.

	[Ni]	NMR Yield (%)
1	(Ph-Xantphos)Ni(II)Br_2	68
2	(Ph-Xantphos)Ni(I)Br	80

Carboxylation of BnZnCl

$$\mathrm{BnZnCl} \xrightarrow[\substack{\text{THF} \\ \text{r.t., 12 hrs.} \\ \textit{then}\ \text{HCl}}]{\substack{CO_2\ \text{(1 atm)} \\ \text{[Ni] (10\%)}}} \mathrm{BnCO_2H}$$

A bomb flask was charged with Ni catalyst (0.010 mmol, 0.1 equiv), evacuated, then refilled with CO_2. Under a stream of CO_2, a solution of BnZnCl (0.10 mmol, 1 equiv) in 2 mL THF was added. The bomb flask was sealed and the reaction mixture was stirred at room temperature for 12 hours. The mixture was quenched with 10%

aqueous HCl and extracted with Et_2O three times. The organic phase was extracted with 10% aqueous KOH three times. The aqueous phase was washed with two portions of Et_2O. The aqueous phase was brought to pH 1 by addition of HCl and extracted with Et_2O three times. Solvent was removed and the residue was dissolved in $CDCl_3$ with 0.5 µL of mesitylene internal standard added for NMR analysis.

	[Ni]	NMR Yield (%)
1	(Ph-Xantphos)Ni(II)Br_2	66
2	No catalyst	0

Carboxylation of *n*-BuZnCl

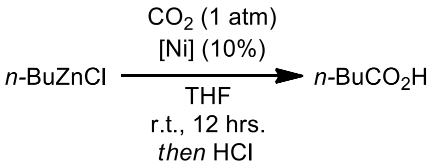

$$n\text{-BuZnCl} \xrightarrow[\substack{\text{THF} \\ \text{r.t., 12 hrs.} \\ \textit{then}\text{ HCl}}]{\substack{CO_2\text{ (1 atm)} \\ \text{[Ni] (10\%)}}} n\text{-BuCO}_2\text{H}$$

A bomb flask was charged with Ni catalyst (0.010 mmol, 0.1 equiv), evacuated, then refilled with CO_2. Under a stream of CO_2, a solution of *n*-BuZnCl (0.10 mmol, 1 equiv) in 2 mL THF was added. The bomb flask was sealed and the reaction mixture was stirred at room temperature for 12 hours. The mixture was quenched with 10% aqueous HCl and extracted with Et_2O three times. The organic phase was extracted with 10% aqueous KOH three times. The aqueous phase was washed with two portions of Et_2O. The aqueous phase was brought to pH 1 by addition of HCl and extracted with Et_2O three times. Solvent was removed and the residue was dissolved in $CDCl_3$ with 0.5 µL of mesitylene internal standard added for NMR analysis.

	[Ni]	NMR Yield (%)
1	(Ph-Xantphos)Ni(II)Br_2	30
2	(Ph-Xantphos)Ni(I)Br	51
3	No catalyst	0

Reductive Carboxylation of BnBr

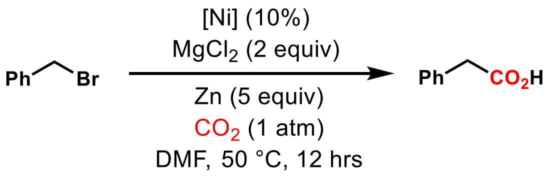

A 25 mL flask was charged with [Ni] (0.024 mmol, 0.1 equiv), $MgCl_2$ (46 mg, 0.48 mmol, 2 equiv), and Zn (79 mg, 1.2 mmol, 5 equiv), then sealed with a septum and purged with CO_2 from a balloon (~0.5 L). DMF (1 mL) and BnBr (29 µL, 0.24 mmol, 1 equiv) were added. A new CO_2 balloon was affixed to the flask and the mixture was stirred vigorously at 50 °C for 12 hours. The mixture was quenched with 10% $HCl_{(aq)}$ and extracted 3 x 5 mL Et_2O. The organic phase was filtered through a plug of Na_2SO_4 and solvent was removed. Solvent was removed and the residue was dissolved in $CDCl_3$ with 0.5 μL of mesitylene internal standard added for NMR analysis.

	[Ni]	NMR Yield (%)
1	(Ph-Xantphos)Ni(II)Br_2	36
2	(*t*-Bu-Xantphos)Ni(I)Br	7
3	No catalyst	0

3. Crystallographic Data

All single crystal data were collected on a Bruker SMART APEXII CCD Diffractometer equipped with an Oxford Cryosystems 700+ Cooler. The x-ray beam generated from a Mo tube was monochromated by a graphite crystal and collimated by an 0.5mm-MonoCap collimator, producing an incident beam at a wavelength of λ(Mo-Kα) = 0.71073 Å. The diffraction data were collected at ω scan methods. All data were processed with the Bruker Apex2 program for unit cell refinement, and data reduction and absorption correction. The structures were solved by the SHELXT program (G. Sheldrick) and refined on F^2 with the SHELXL (G. Sheldrick). Non-hydrogen atoms were refined with anisotropic displacement parameters and hydrogen atoms on carbons were placed in idealized positions (C-H = 0.95 or 0.99 Å) and included as riding with U_{iso}(H) = 1.2 U_{eq}(non-H). Crystallographic data of these structures including cif, fcf, and hkl files have been deposited with the Cambridge Crystallographic Data Centre with the numbers of 1869808-1869816. Copies of these data can be requested from, free of charge, the CCDC website at https://www.ccdc.cam.ac.uk/structures/.

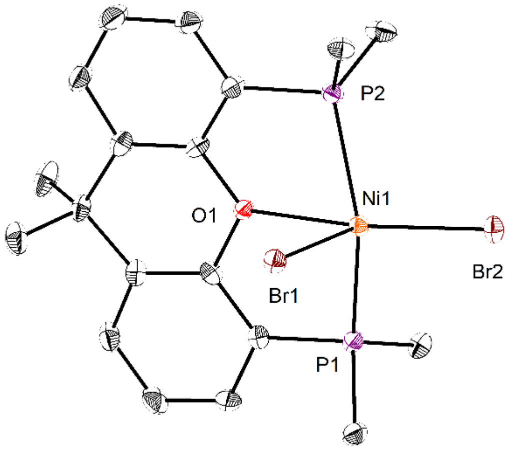

Figure S1. X-ray structure of **1** at 50% probability thermal ellipsoids. Hydrogen atoms are omitted and *t*-Bu groups are truncated to Me groups for clarity. Selected atomic distances: Ni–O = 2.3886(15) Å; Ni–Br1 = 2.4071(7) Å; Ni–Br2 = 2.4379(5) Å.

(*t*-BuXantphos)Ni(II)Br$_2$ (1)

Formula: $C_{31}H_{48}Br2NiOP_2$, M_r = 717.12, dark purple rod, 0.110 x 0.140 x 0.400 mm^3, space group *P 42/n*, *a* = 23.382(3) Å, *b* = 23.382(3) Å, *c* = 11.9926(16) Å, β = 90°, *V* = 6556.6(19) Å^3 , *Z* = 8, ρ_{calcd} = 1.453 g/cm^3 , μ = 3.149 mm^{-1}, *F*(000) = 2960.0, *T* = 100(2) K, R_1 = 0.0320, wR^2 = 0.0775, 8147 independent reflections.

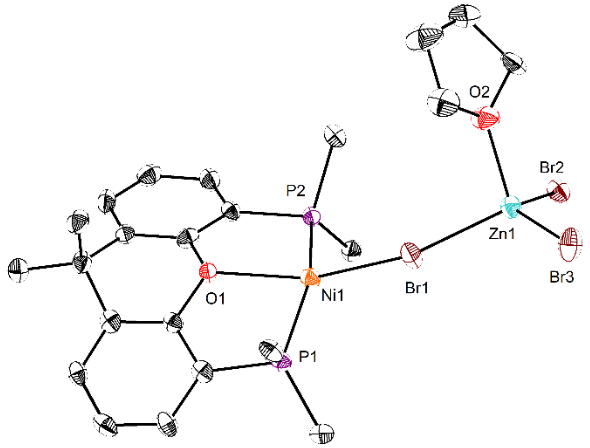

Figure S2. X-ray structure of **2** at 50% probability thermal ellipsoids. Hydrogen atoms are omitted and *t*-Bu groups are truncated to Me groups for clarity. Independent molecule of **3** omitted for clarity. Selected atomic distances: Ni1–O1 = 2.2910(38) Å; Ni1–Br1 = 2.6329(10) Å; Zn1–Br1 = 2.4488(9) Å.

(*t*-BuXantphos)NiBr·ZnBr$_2$(THF) + (*t*-BuXantphos)NiBr (2)

Formula: $C_{66}H_{104}Br_4Ni_2O_3P_4Zn$, M_r = 1571.80, yellow plate, 0.030 x 0.120 x 0.180 mm^3, space group *P 1 21 1*, *a* = 11.3264(16) Å, *b* = 15.593(2) Å, *c* = 19.952(3) Å, β = 102.789(2)°, *V* = 3436.4(8) Å^3 , *Z* = 2, ρ_{calcd} = 1.519 g/cm^3 , μ = 3.350 mm^{-1}, *F*(000) = 1620, *T* = 100(2) K, R_1 = 0.0368, wR^2 = 0.0753, 14058 independent reflections.

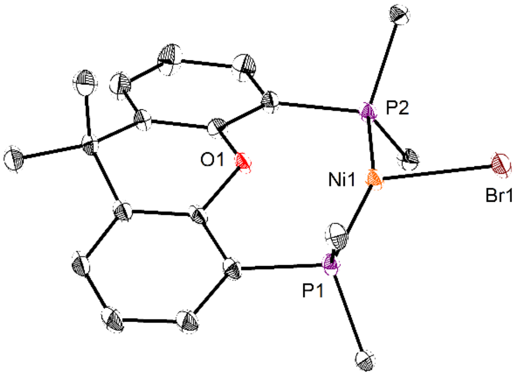

Figure S3. X-ray structure of **3** at 50% probability thermal ellipsoids. Hydrogen atoms are omitted and *t*-Bu groups are truncated to Me groups for clarity. Ni–O = 2.4339(15) Å; Ni–Br = 2.4650(5) Å.

(*t*-BuXantphos)NiBr (3)

Formula: $C_{31}H_{48}BrNiOP_2$, M_r = 637.26, yellow rod, 0.110 x 0.120 x 0.540 mm^3, space group *P 21/c*, a = 11.1629(9) Å, b = 16.8436(13) Å, c = 17.3026(13) Å, β = 105.4486(13)°, V = 3135.8(4) Å^3 , Z = 4, ρ_{calcd} = 1.350 g/cm^3 , μ = 2.017 mm^{-1}, F(000) = 1340.0, T = 100(2) K, R_1 = 0.0394, wR^2 = 0.0947, 7784 independent reflections.

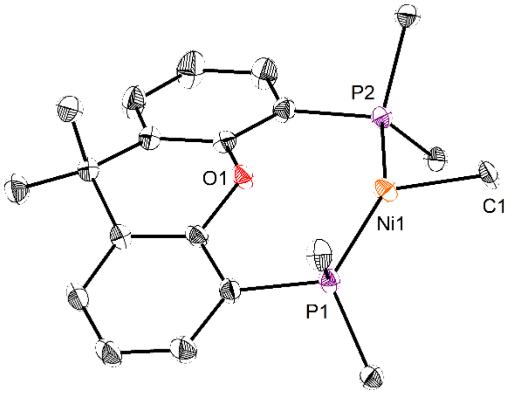

Figure S4. X-ray structure of **4** at 50% probability thermal ellipsoids. Hydrogen atoms are omitted and *t*-Bu groups are truncated to Me groups for clarity. Ni1–O1 = 2.6018(11) Å; Ni1–C1 = 2.0543(84) Å.

(*t*-BuXantphos)Ni(I)Me (4)

Formula: $C_{32}H_{52}NiOP_2$, M_r = 573.40, brown plate, 0.080 x 0.460 x 0.480 mm^3, space group *P 1 21/c 1*, a = 11.2386(5) Å, b = 16.7163(8) Å, c = 17.2831(8) Å, β = 105.0036(7)°, V = 3136.2(3) Å^3 , Z = 4, ρ_{calcd} = 1.235 g/cm^3 , μ = 0.955 mm^{-1}, F(000) = 1253, T = 100(2) K, R_1 = 0.0344, wR^2 = 0.0857, 7780 independent reflections.

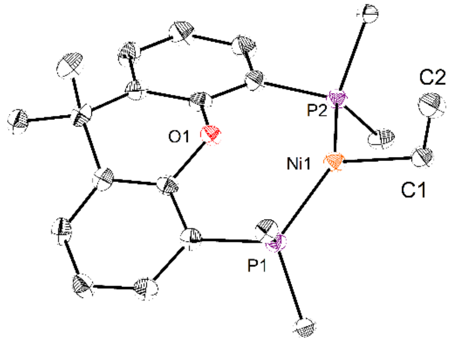

Figure S5. X-ray structure of **5** at 50% probability thermal ellipsoids. Hydrogen atoms are omitted and *t*-Bu groups are truncated to Me groups for clarity. Ni1–O1 = 2.6737(16) Å; Ni1–C1 = 2.0335(24) Å; C1–C2 = 1.5422(33) Å.

(*t*-BuXantphos)Ni(I)Et (5)

Formula: $C_{33}H_{53}NiOP_2$, M_r = 586.40, brown plate, 0.020 x 0.180 x 0.210 mm^3, space group *P 1 21/c 1*, *a* = 11.4841(10) Å, *b* = 16.0721(14) Å, *c* = 17.5988(15) Å, β = 98.980(2) °, *V* = 3208.5(5) Å^3 , *Z* = 4, ρ_{calcd} = 1.214 g/cm^3 , μ = 0.727 mm^{-1}, *F*(000) = 1268, *T* = 100(2) K, R_1 = 0.0414, wR^2 = 0.1040, 6575 independent reflections.

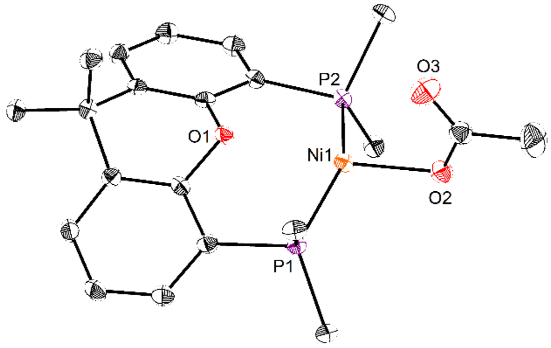

Figure S6. X-ray structure of **9** at 50% probability thermal ellipsoids. Hydrogen atoms are omitted and *t*-Bu groups are truncated to Me groups for clarity. Ni1–O1 = 2.4707(12) Å; Ni1–O2 = 2.0146(14) Å.

(*t*-BuXantphos)Ni(I)OAc (9)

Formula: $C_{33}H_{51}NiO_3P_2$, M_r = 717.12, orange rod, 0.060 x 0.090 x 0.430 mm^3, space group *P 1 21/c 1*, *a* = 12.3675(16) Å, *b* = 12.1650(16) Å, *c* = 22.968(3) Å, β = 102.160(2)°, *V* = 3378.0(8) Å^3 , *Z* = 4, ρ_{calcd} = 1.212 g/cm^3 , μ = 0.699 mm^{-1}, *F*(000) = 1324, *T* = 100(2) K, R_1 = 0.0392, wR^2 = 0.0947 8402 independent reflections.

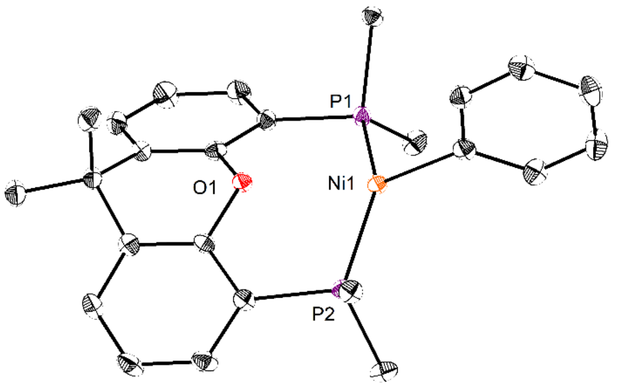

Figure S7. X-ray structure of **11** at 50% probability thermal ellipsoids. Hydrogen atoms are omitted and *t*-Bu groups are truncated to Me groups for clarity. Selected atomic distances: Ni–O = 2.5184(10) Å; Ni–C = 1.9795(19) Å.

(*t*-BuXantphos)NiPh (11)

Formula: $C_{37}H_{53}NiOP_2$, M_r = 634.42, brown block, 0.110 x 0.260 x 0.340 mm^3, space group *P 21/n*, *a* = 12.1524(4) Å, *b* = 25.0770(9) Å, *c* = 12.2188(4) Å, β = 113.4946(5)°, *V* = 3414.9(2) Å^3 , *Z* = 4, ρ_{calcd} = 1.234 g/cm^3, μ = 0.689 mm^{-1}, *F*(000) = 1364, *T* = 100(2) K, R_1 = 0.0347, wR^2 = 0.0895, 8480 independent reflections.

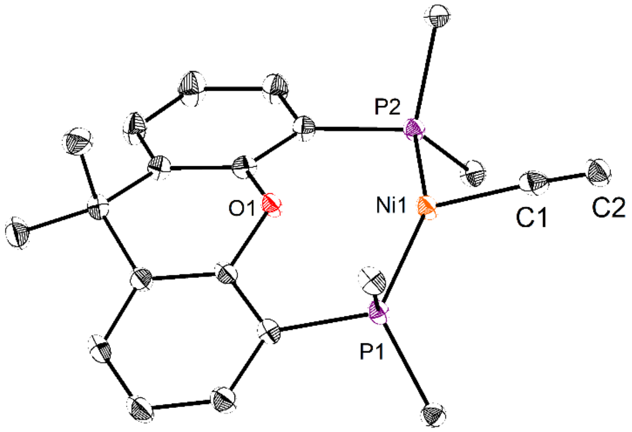

Figure S8. X-ray structure of **6** at 50% probability thermal ellipsoids. Hydrogen atoms are omitted and *t*-Bu groups are truncated to Me groups for clarity. Selected atomic distances: Ni–O1 = 2.5405(11) Å; Ni–C1 = 1.9359(15) Å; C1–C2 = 1.1937(20) Å.

(*t*-BuXantphos)Ni-Acetylide(6)

Formula: $C_{33}H_{49}NiOP_2$, M_r = 582.38, red/orange block, 0.130 x 0.290 x 0.380 mm^3, space group *P 1 21/c 1*, *a* = 11.0939(12) Å, *b* = 16.9554(19) Å, *c* = 17.5168(19) Å, β = 105.2295(16) °, *V* = 3179.2(6) Å^3 , *Z* = 4, ρ_{calcd} = 1.217 g/cm^3, μ = 0.734 mm^{-1}, *F*(000) = 1252, *T* = 100(2) K, R_1 = 0.0331, wR^2 = 0.0849, 7900 independent reflections.

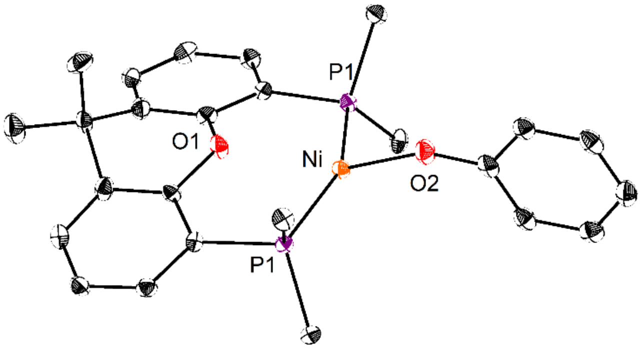

Figure S9. X-ray structure of **8** at 50% probability thermal ellipsoids. Hydrogen atoms are omitted and *t*-Bu groups are truncated to Me groups for clarity. Ni1–O1 = 2.5250(31) Å; Ni1–O2 = 1.9635(31) Å.

(*t*-BuXantphos)Ni(I)OPh (8)

Formula: $C_{37}H_{53}NiO_2P_2$, M_r = 650.44, yellow prism, 0.170 x 0.210 x 0.310 mm^3, space group *P m n 21*, *a* = 14.3403(6) Å, *b* = 15.0020(6) Å, *c* = 16.2605(7) Å, β = 90°, *V* = 3498.2(3) Å^3 , *Z* = 4, ρ_{calcd} = 1.235 g/cm^3 , μ = 0.676 mm^{-1}, *F*(000) = 1396, *T* = 100(2) K, R_1 = 0.0351, wR^2 = 0.0834, 9023 independent reflections.

4. NMR, IR, and UV-Vis Spectra

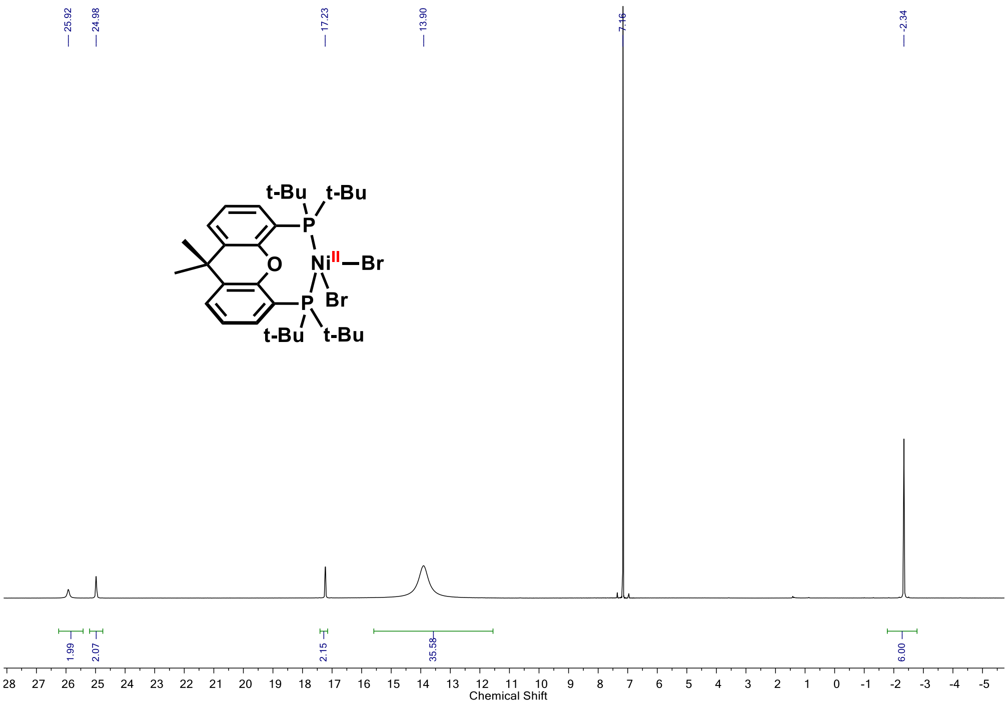

Figure S10. ^{1}H NMR (400 MHz, C_6D_6, 25 °C) of **1**.

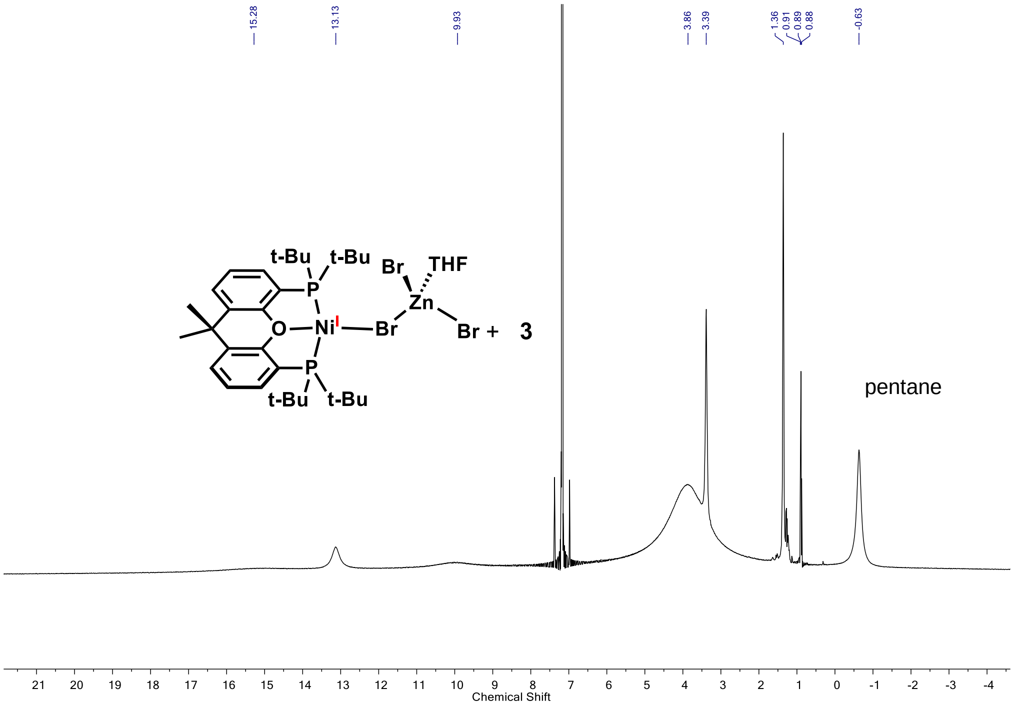

Figure S11. ^{1}H NMR (400 MHz, C_6D_6, 25 °C) of **2**.

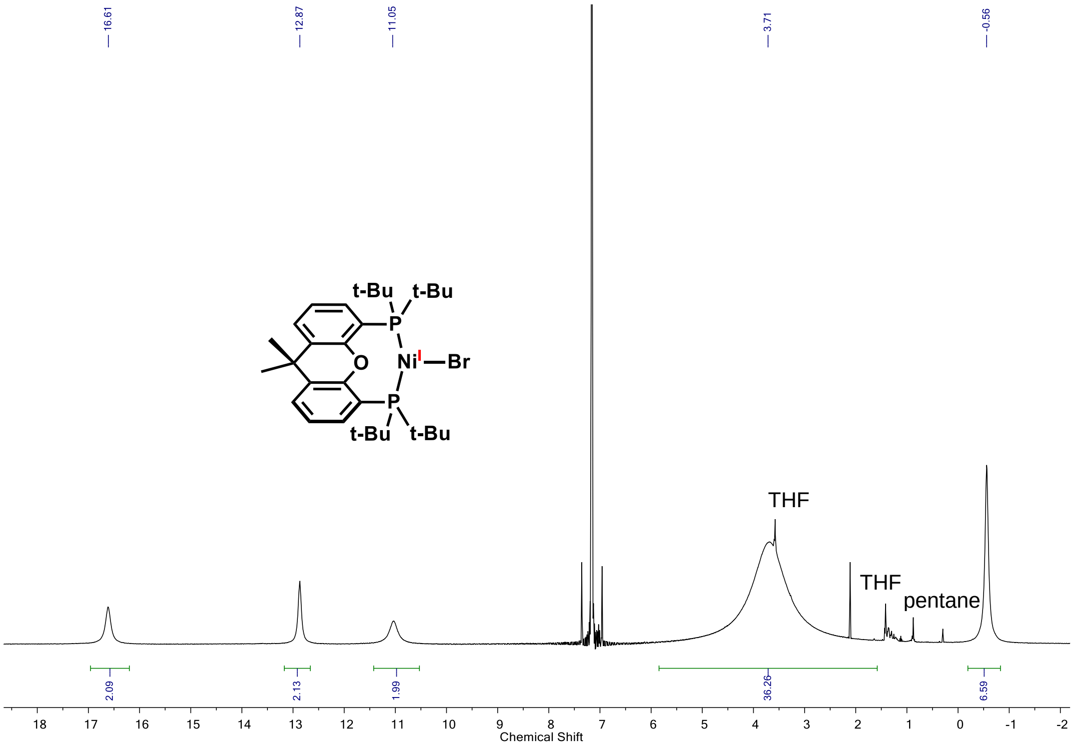

Figure S12. ^{1}H NMR (400 MHz, C_6D_6, 25 °C) of **3**.

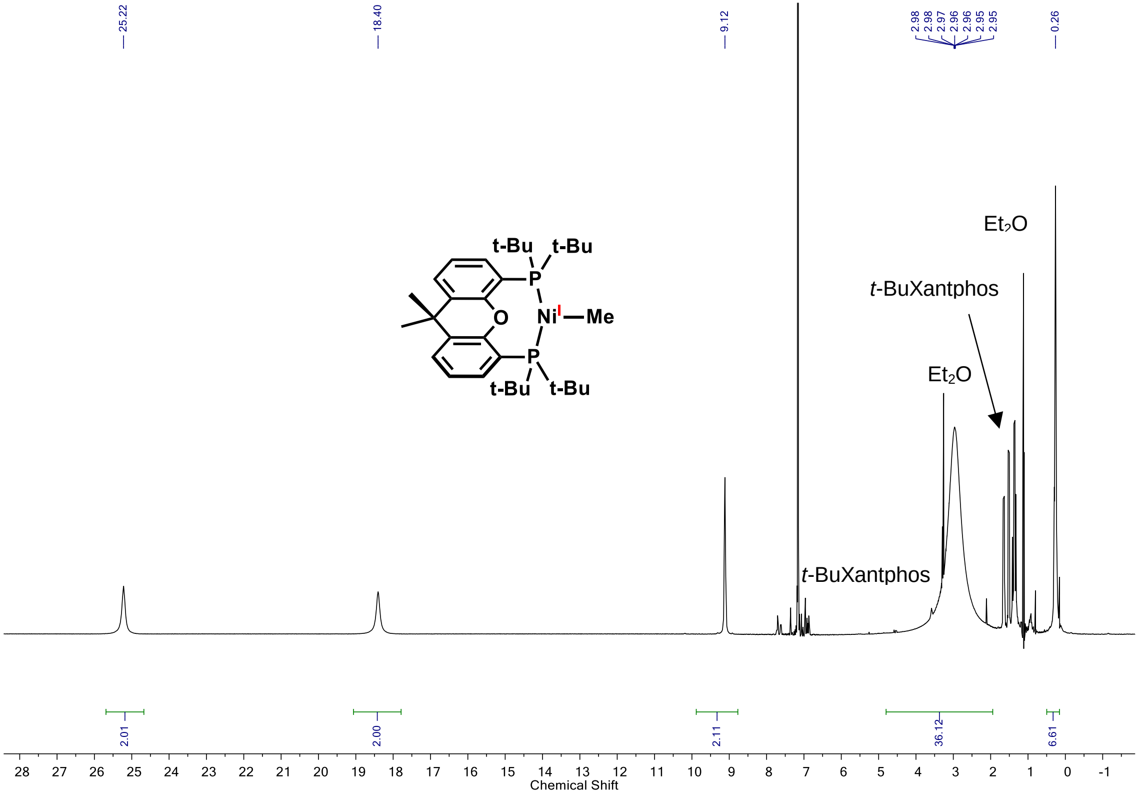

Figure S13. ^{1}H NMR (400 MHz, C_6D_6, 25 °C) of **4**.

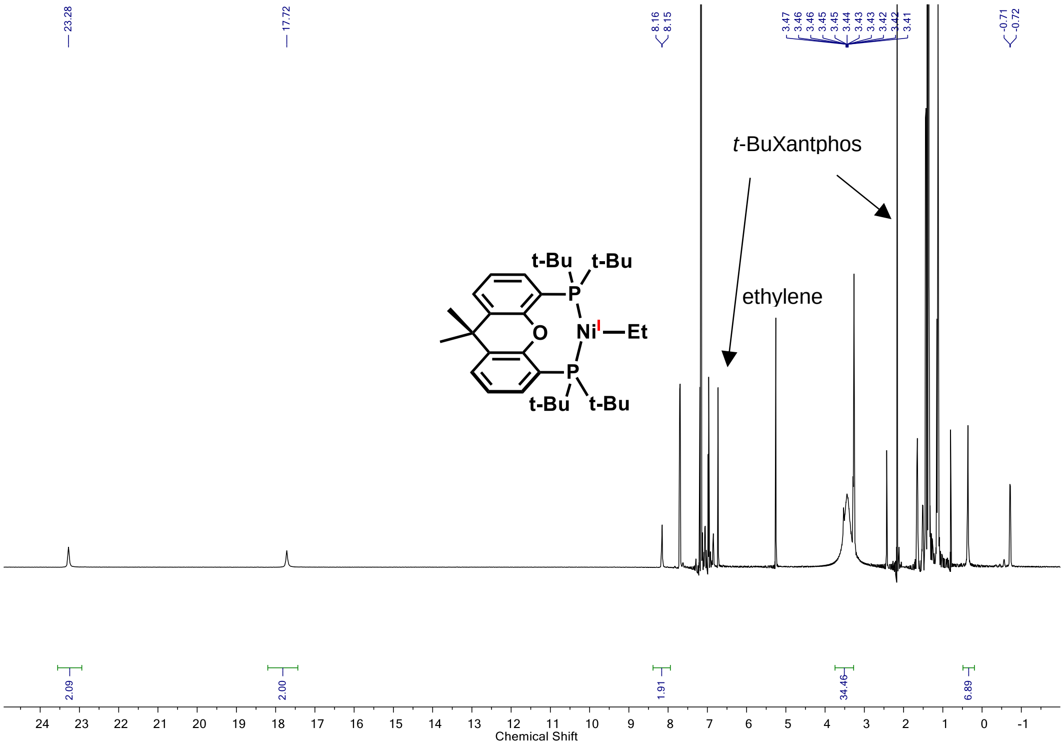

Figure S14. ^{1}H NMR (400 MHz, C_6D_6, 25 °C) of **5**.

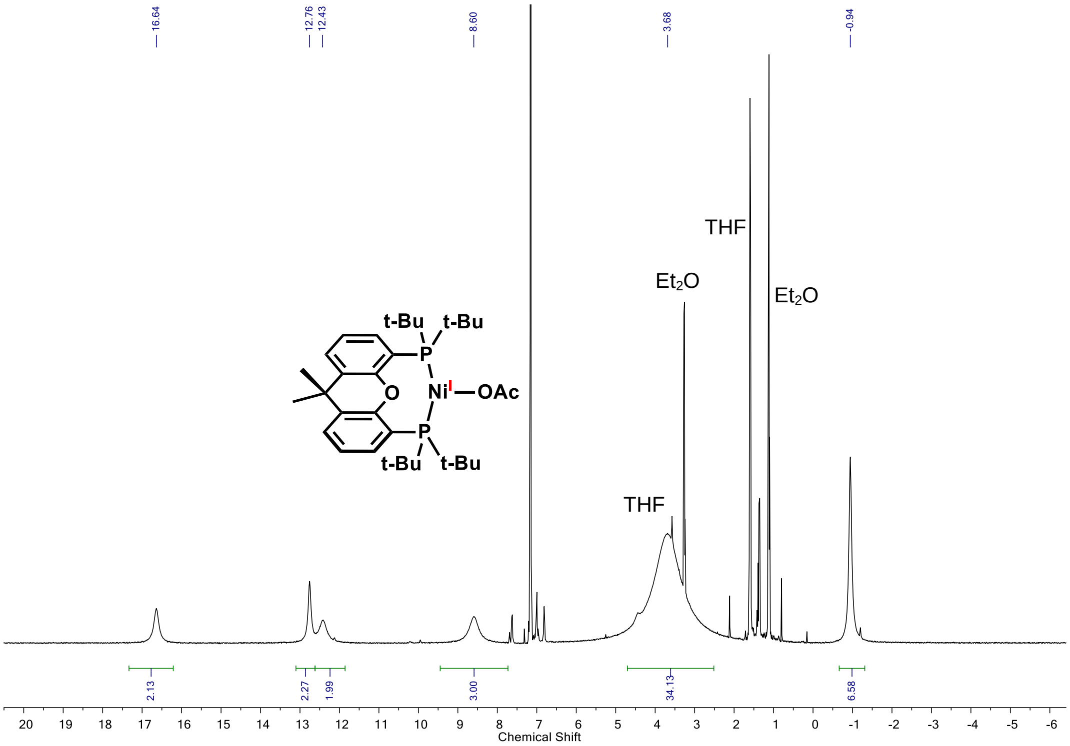

Figure S15. ^{1}H NMR (400 MHz, C_6D_6, 25 °C) of **9**.

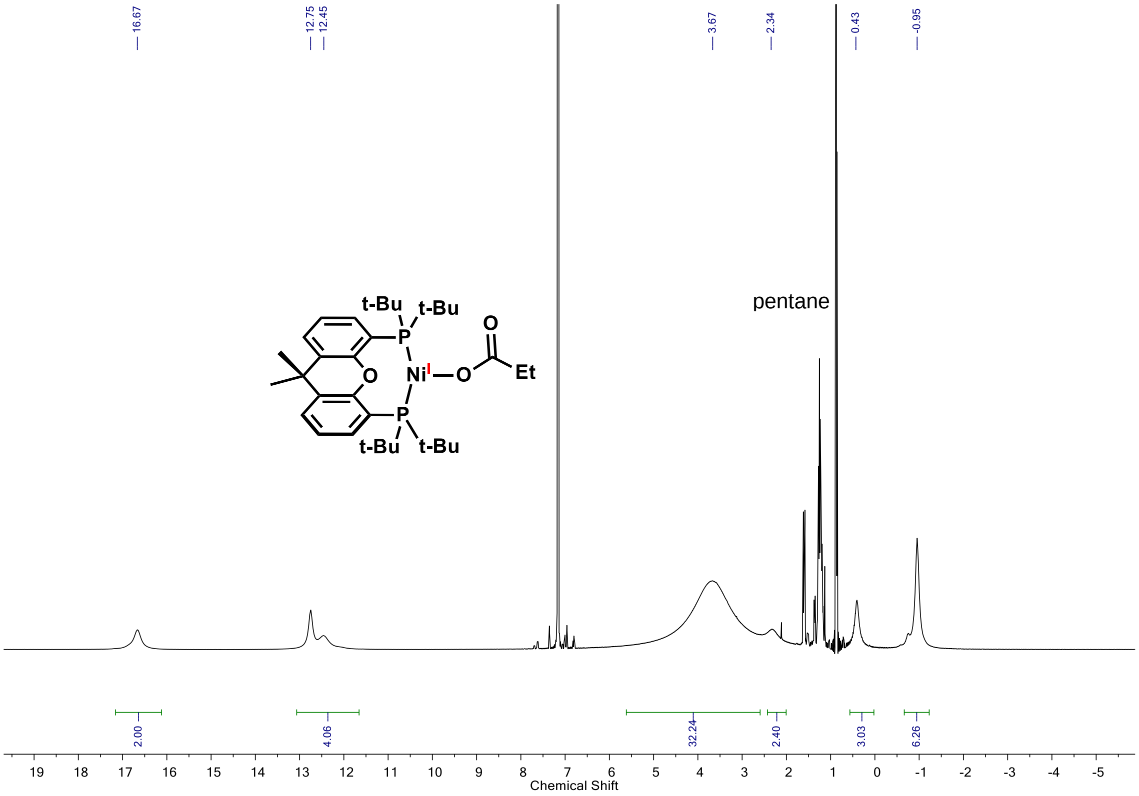

Figure S16. ^{1}H NMR (400 MHz, C_6D_6, 25 °C) of **10**.

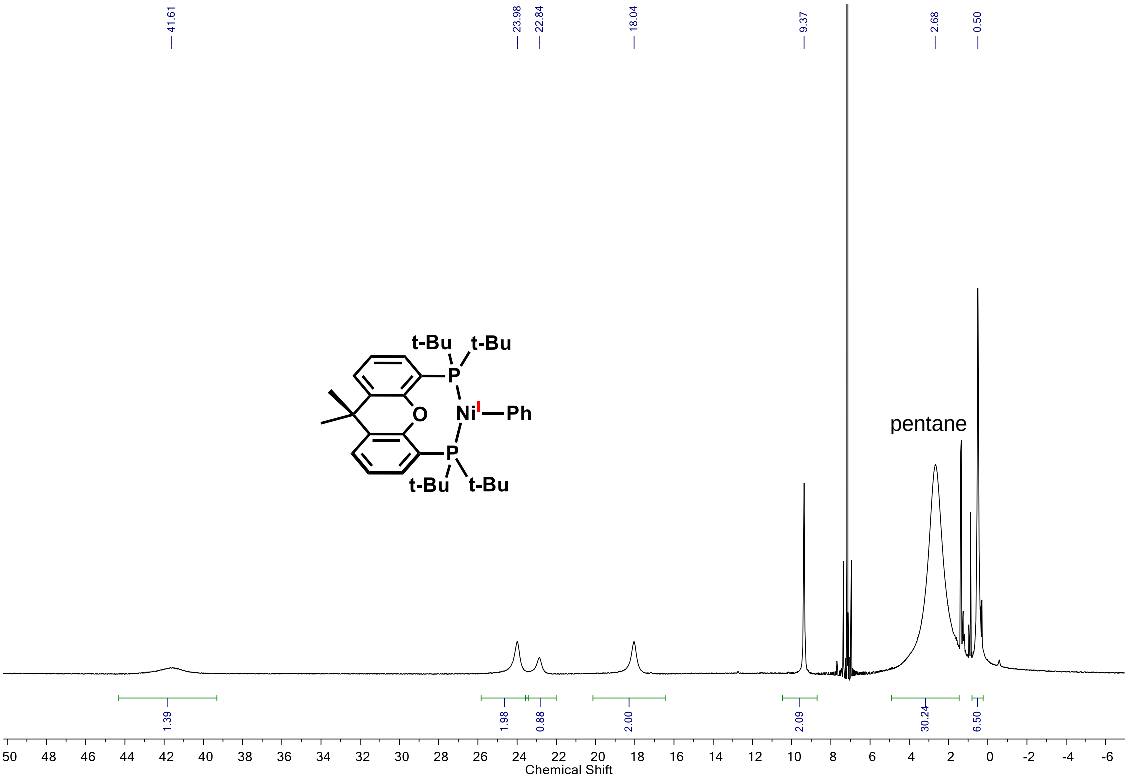

Figure S17. ^{1}H NMR (400 MHz, C_6D_6, 25 °C) of **11**.

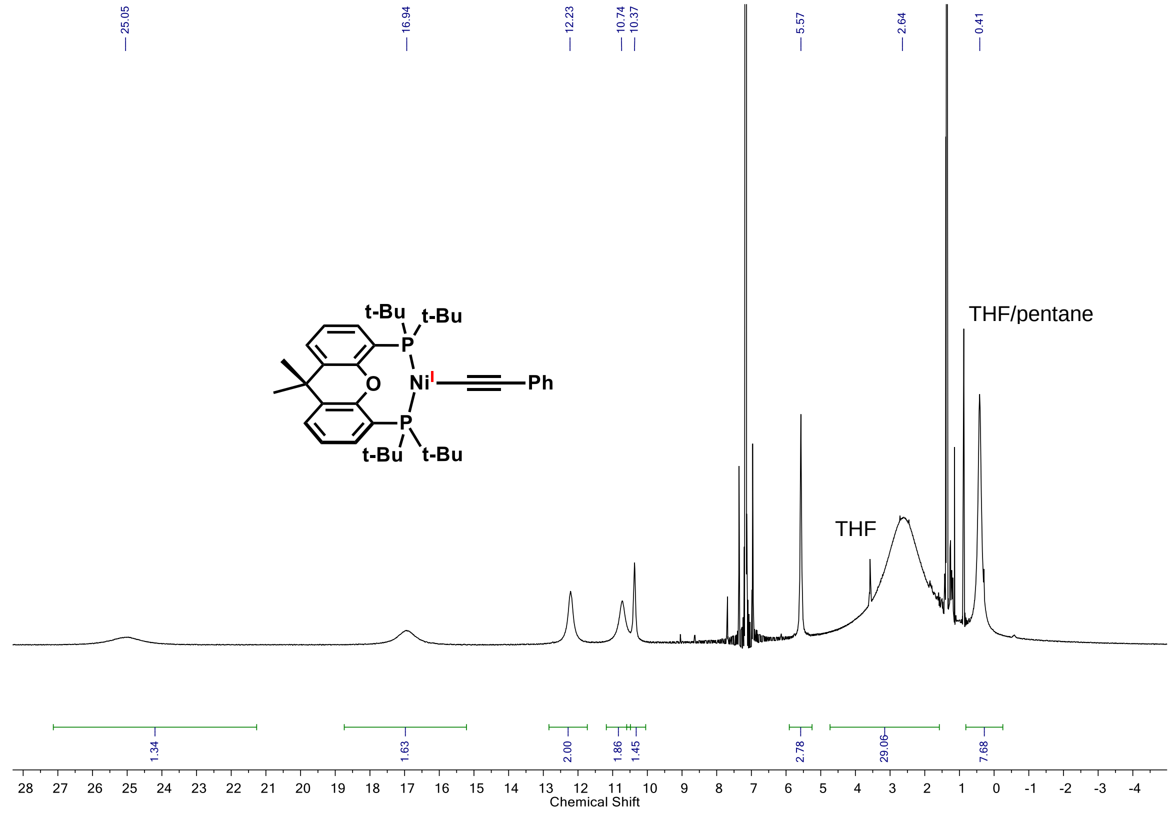

Figure S18. ^{1}H NMR (400 MHz, C_6D_6, 25 °C) of **7**.

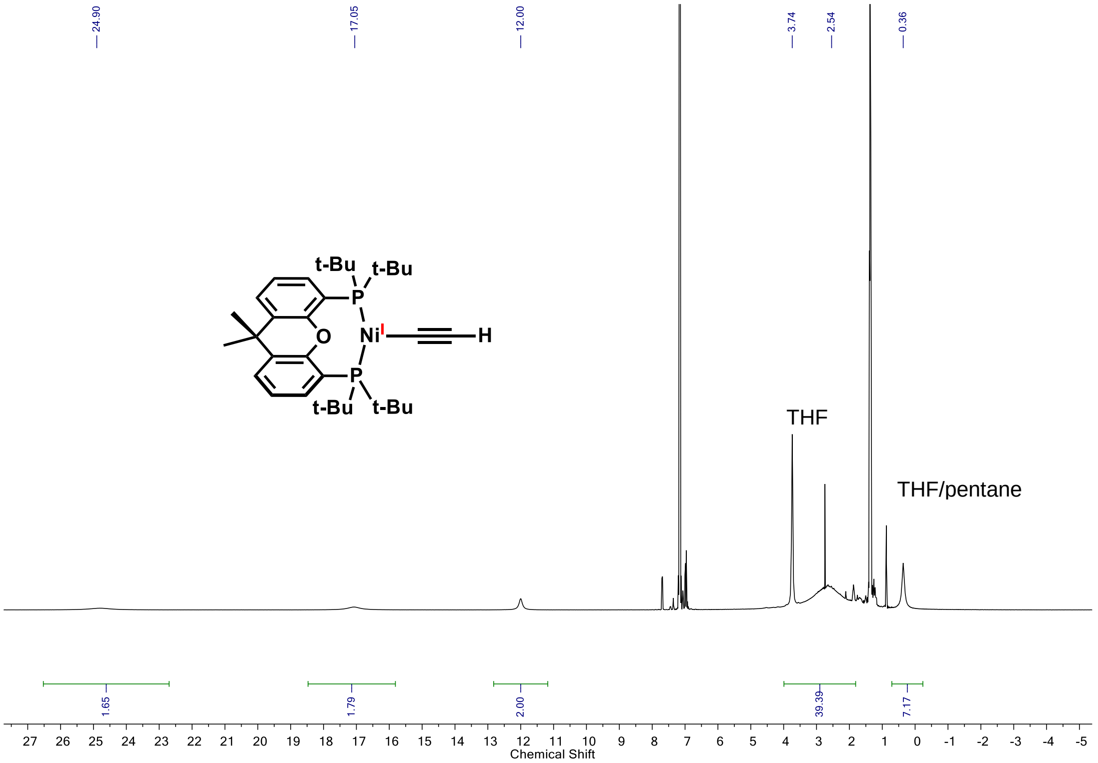

Figure S19. ^{1}H NMR (400 MHz, C_6D_6, 25 °C) of **6**.

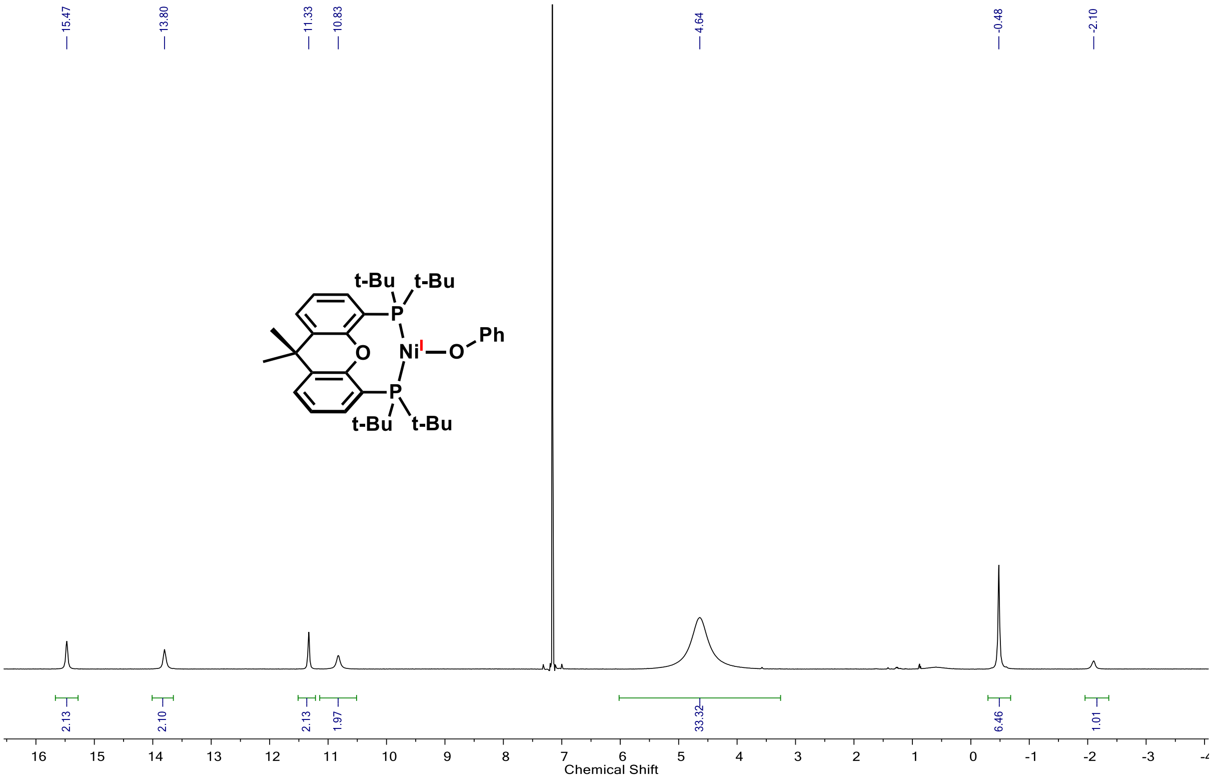

Figure S20. ^{1}H NMR (400 MHz, C_6D_6, 25 °C) of **8**.

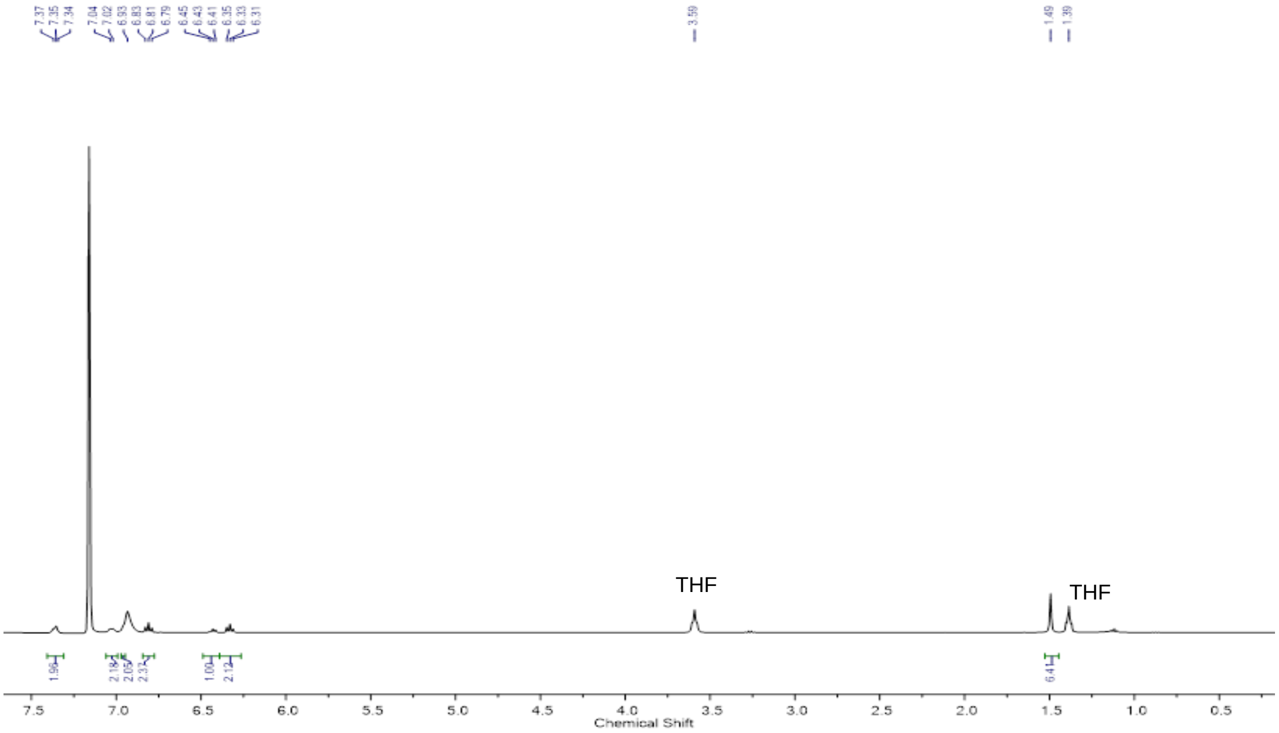

Figure S21. ^{1}H NMR (400 MHz, C_6D_6, 25 °C) of (Ph-Xantphos)Ni(II)BrPh

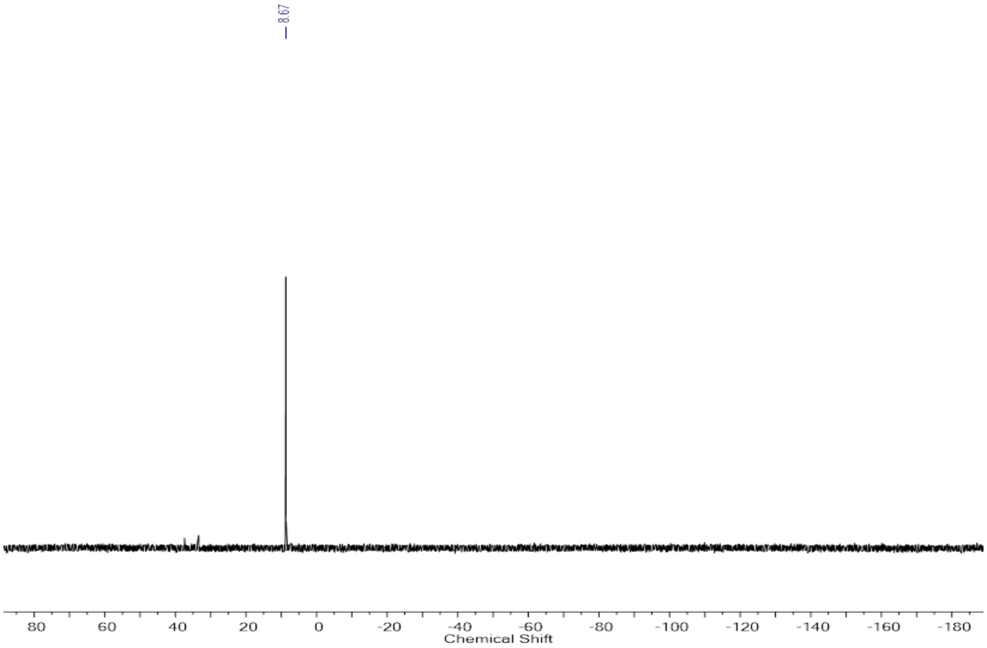

Figure S22. ^{31}P NMR (162 MHz, C_6D_6, 25 °C) of (Ph-Xantphos)Ni(II)BrPh

IR Spectra

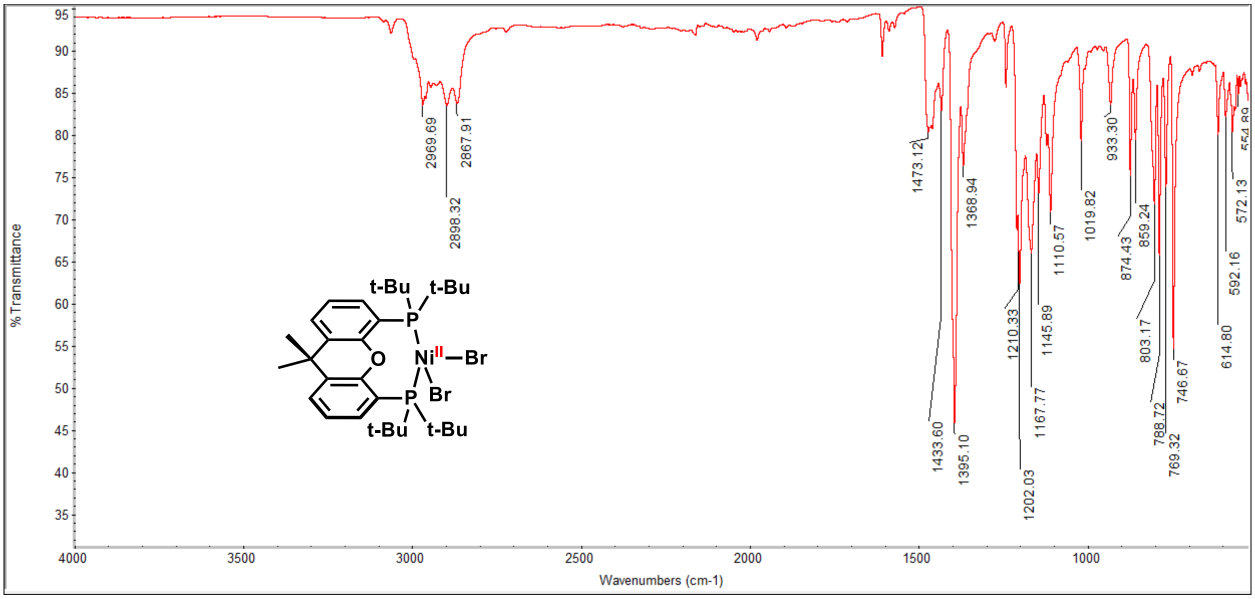

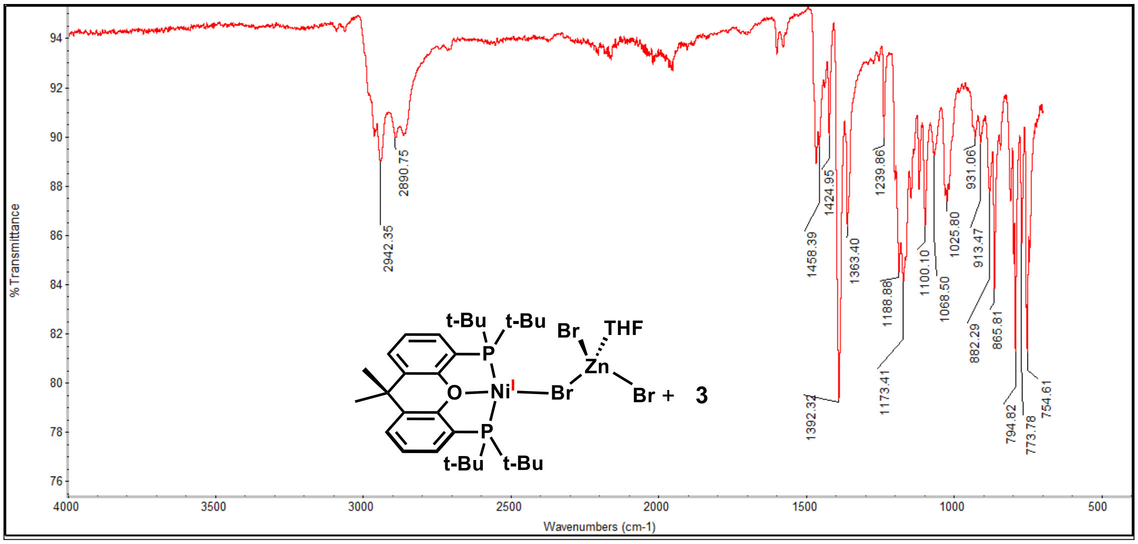
% Transmittance
94
92
90
88
86
84
82
80
78
76
4000
3500
3000
2500
2000
1500
1000
500
Wavenumbers (cm-1)
2942.35
2890.75
1458.39
1424.95
1392.32
1363.40
1239.86
1188.88
1173.41
1100.10
1068.50
1025.80
931.06
913.47
882.29
865.81
794.82
773.78
754.61
t-Bu
t-Bu
P
O
Ni^I
Br
P
t-Bu
t-Bu
Br
THF
Zn
Br +
3

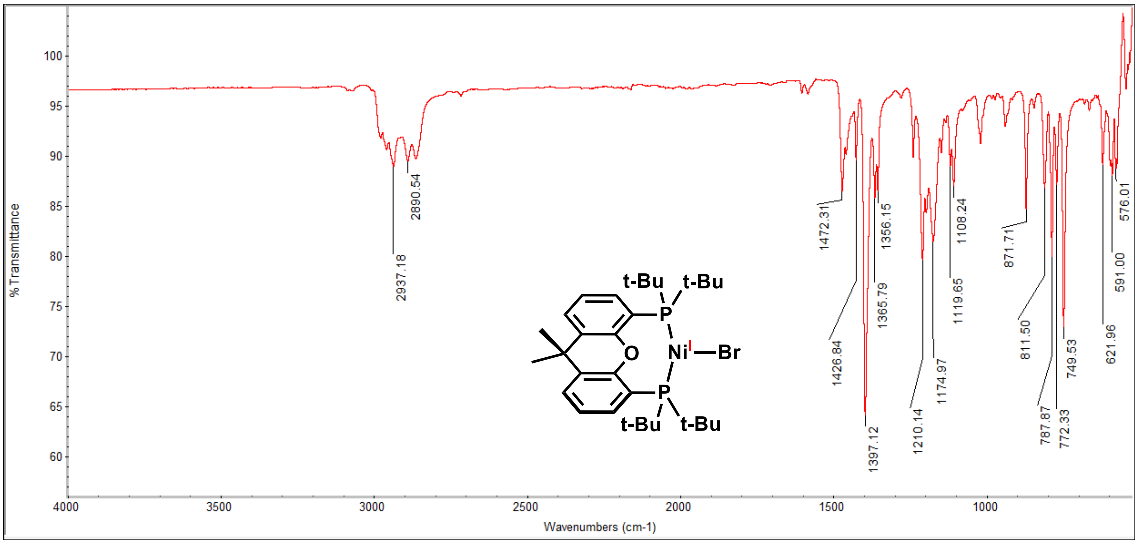
% Transmittance
100
95
90
85
80
75
70
65
60
4000
3500
3000
2500
2000
1500
1000
Wavenumbers (cm-1)
2937.18
2890.54
1472.31
1426.84
1397.12
1365.79
1356.15
1210.14
1174.97
1119.65
1108.24
871.71
811.50
787.87
772.33
749.53
621.96
591.00
576.01
t-Bu
t-Bu
P
O
Ni^I
Br
P
t-Bu
t-Bu

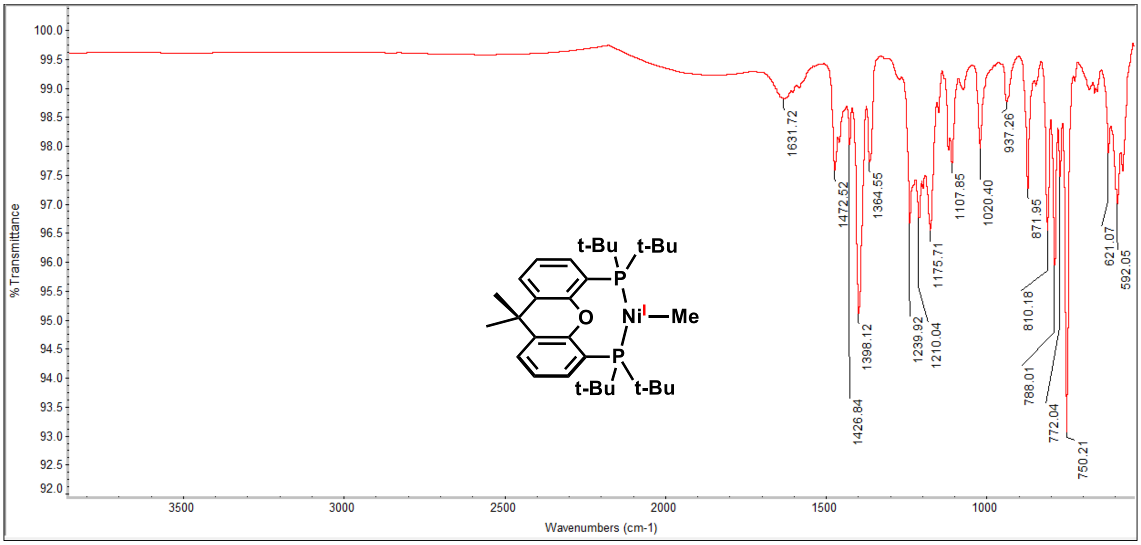
% Transmittance
100.0
99.5
99.0
98.5
98.0
97.5
97.0
96.5
96.0
95.5
95.0
94.5
94.0
93.5
93.0
92.5
92.0
3500
3000
2500
2000
1500
1000
Wavenumbers (cm-1)
1631.72
1472.52
1426.84
1398.12
1364.55
1239.92
1210.04
1175.71
1107.85
1020.40
937.26
871.95
810.18
788.01
772.04
750.21
621.07
592.05
t-Bu
t-Bu
P
O
Ni^I
Me
P
t-Bu
t-Bu

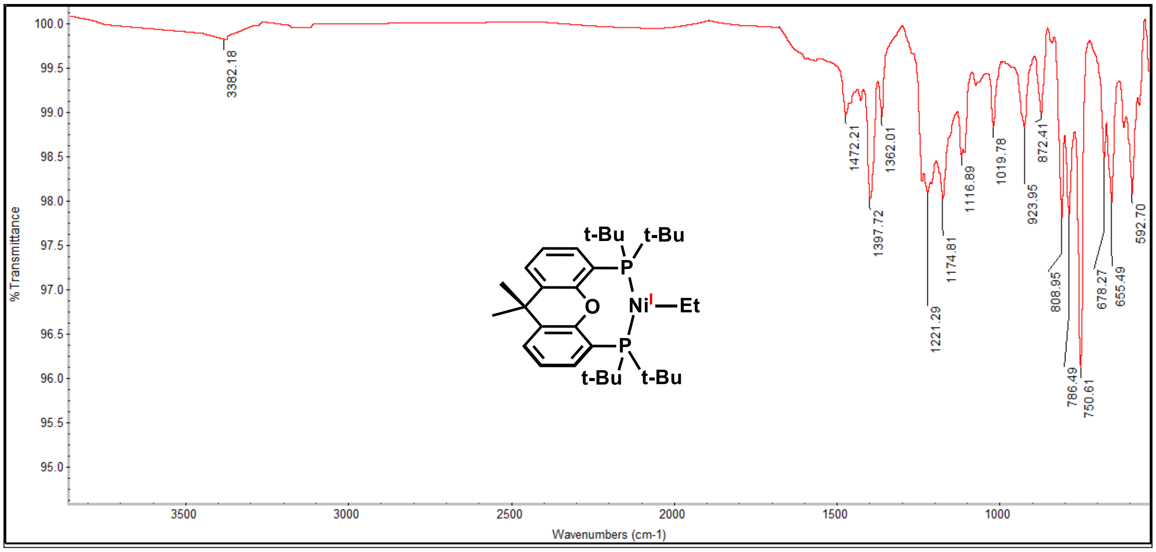

100.0
99.5
99.0
98.5
98.0
97.5
97.0
96.5
96.0
95.5
95.0
% Transmittance
3500
3000
2500
2000
1500
1000
Wavenumbers (cm-1)
3382.18
1472.21
1397.72
1362.01
1221.29
1174.81
1116.89
1019.78
923.95
872.41
808.95
786.49
750.61
678.27
655.49
592.70
t-Bu
t-Bu
P
O
Ni^I
Et
P
t-Bu
t-Bu

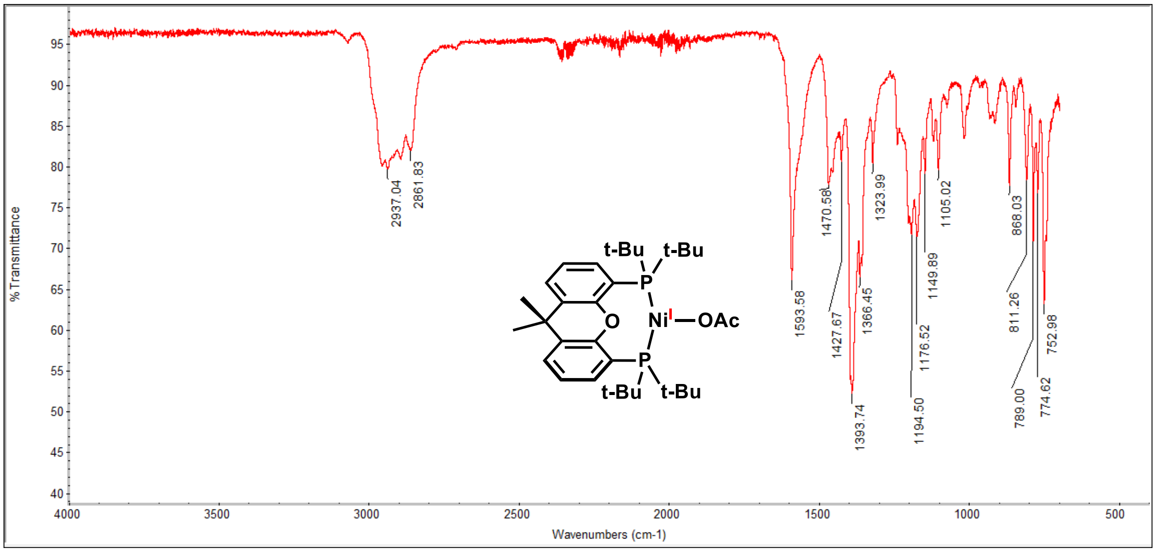

95
90
85
80
75
70
65
60
55
50
45
40
% Transmittance
4000
3500
3000
2500
2000
1500
1000
500
Wavenumbers (cm-1)
2937.04
2861.83
1593.58
1470.58
1427.67
1393.74
1366.45
1323.99
1194.50
1176.52
1149.89
1105.02
868.03
811.26
789.00
774.62
752.98
t-Bu
t-Bu
P
O
Ni^I
OAc
P
t-Bu
t-Bu

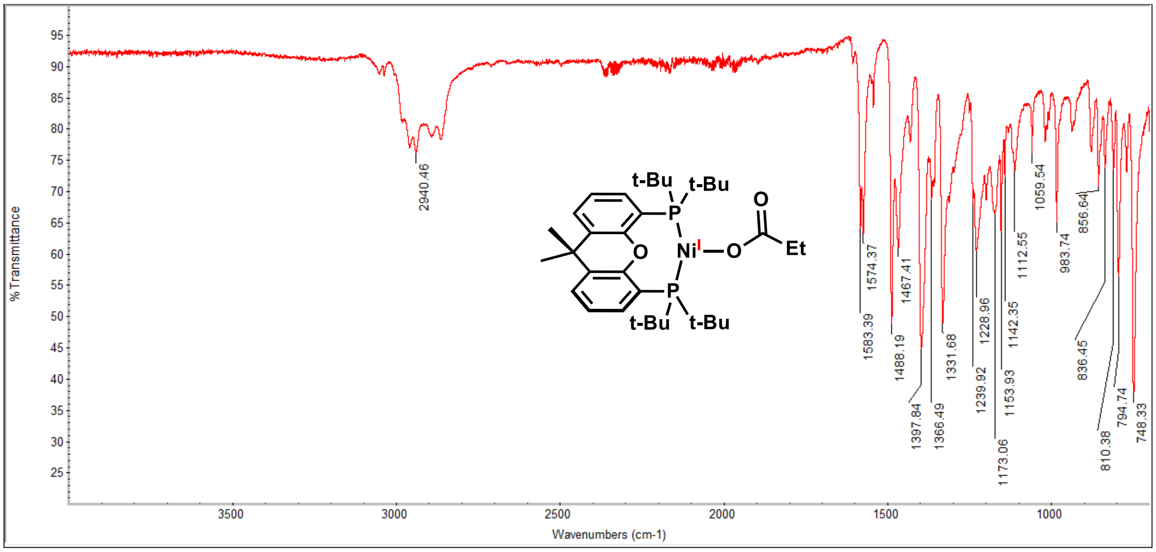

95
90
85
80
75
70
65
60
55
50
45
40
35
30
25
% Transmittance
3500
3000
2500
2000
1500
1000
Wavenumbers (cm-1)
2940.46
1583.39
1574.37
1488.19
1467.41
1397.84
1366.49
1331.68
1239.92
1228.96
1173.06
1153.93
1142.35
1112.55
1059.54
983.74
856.64
836.45
810.38
794.74
748.33
t-Bu
t-Bu
P
O
Ni^I
O
O
Et
P
t-Bu
t-Bu

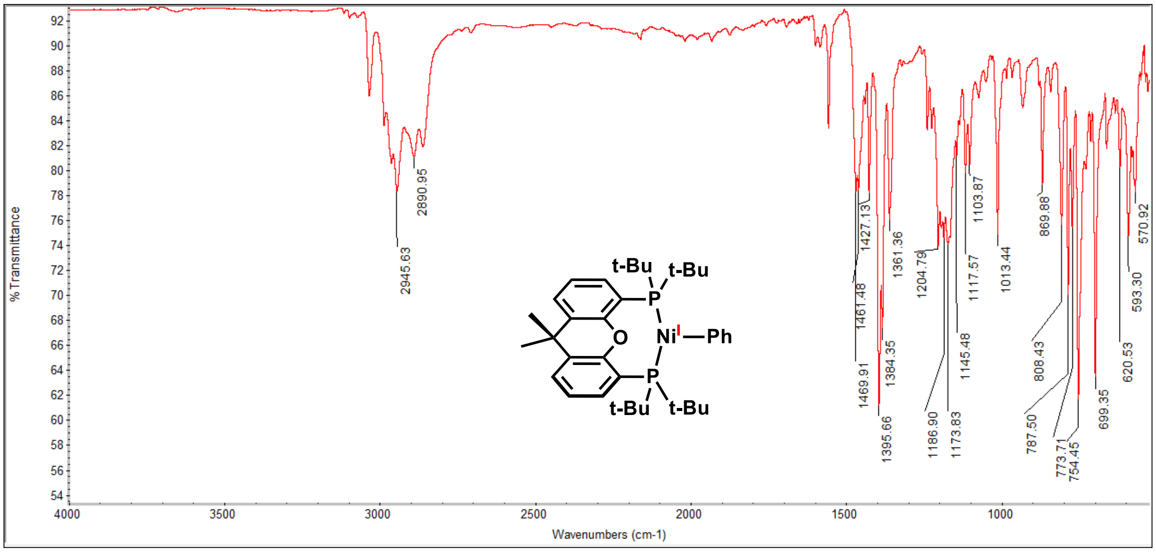
% Transmittance
Wavenumbers (cm-1)
4000
3500
3000
2500
2000
1500
1000
92
90
88
86
84
82
80
78
76
74
72
70
68
66
64
62
60
58
56
54
2945.63
2890.95
1469.91
1461.48
1427.13
1395.66
1384.35
1361.36
1204.79
1186.90
1173.83
1145.48
1117.57
1103.87
1013.44
869.88
808.43
787.50
773.71
754.45
699.35
620.53
593.30
570.92
t-Bu
t-Bu
P
O
Ni^I
Ph
P
t-Bu
t-Bu

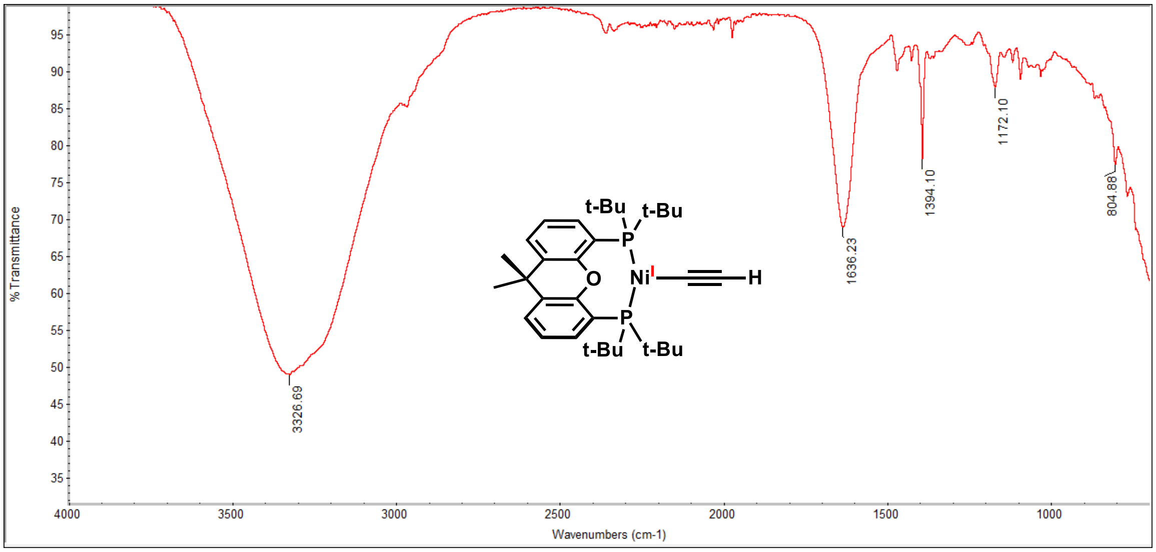
% Transmittance
Wavenumbers (cm-1)
4000
3500
3000
2500
2000
1500
1000
95
90
85
80
75
70
65
60
55
50
45
40
35
3326.69
1636.23
1394.10
1172.10
804.88
t-Bu
t-Bu
P
O
Ni^I
H
P
t-Bu
t-Bu

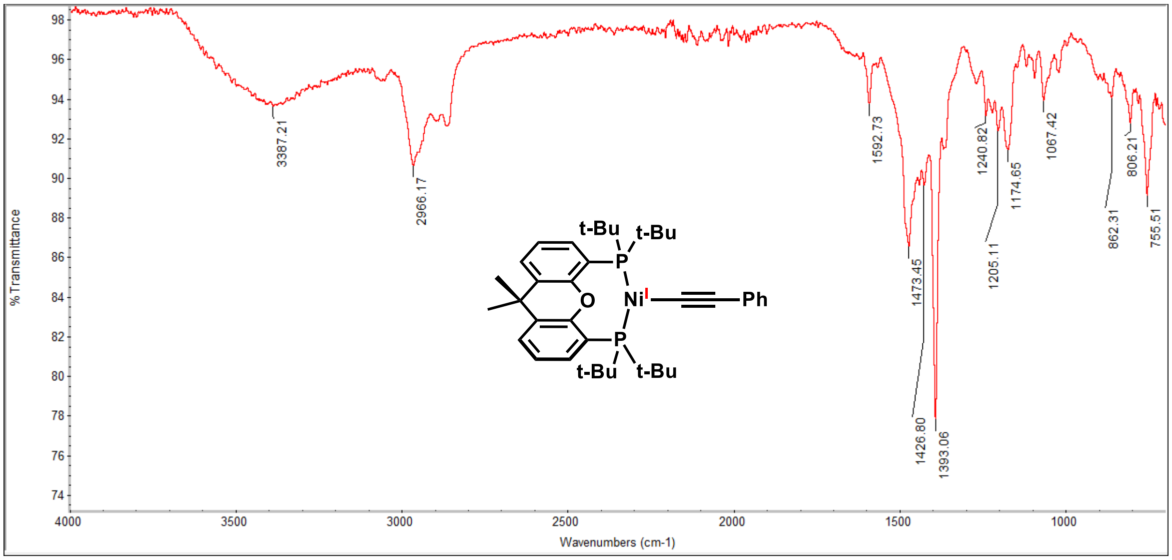
% Transmittance
Wavenumbers (cm-1)
4000
3500
3000
2500
2000
1500
1000
98
96
94
92
90
88
86
84
82
80
78
76
74
3387.21
2966.17
1592.73
1473.45
1426.80
1393.06
1240.82
1205.11
1174.65
1067.42
862.31
806.21
755.51
t-Bu
t-Bu
P
O
Ni^I
Ph
P
t-Bu
t-Bu

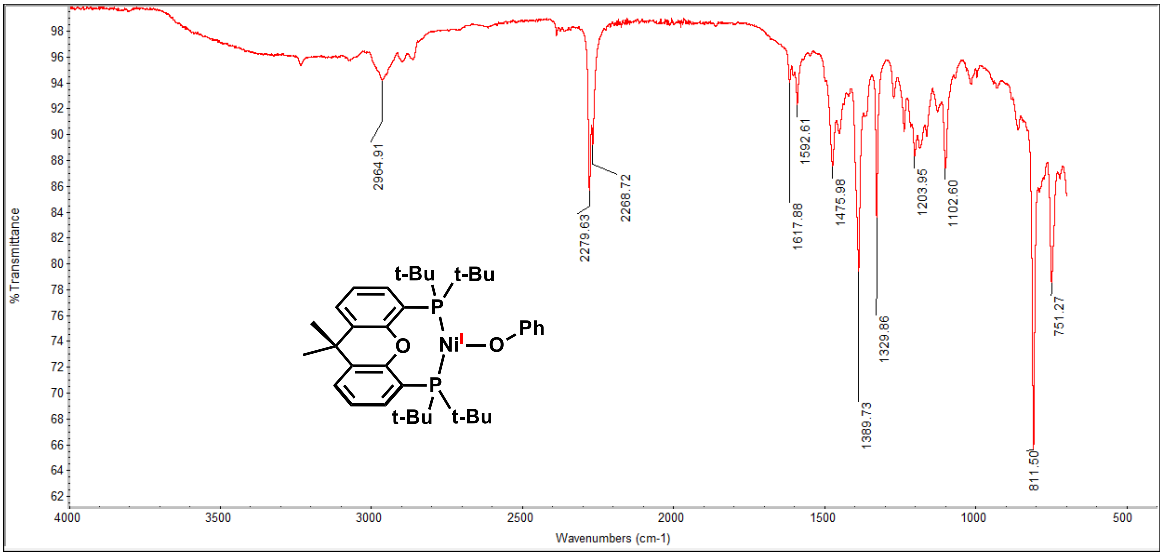

UV-Vis Spectra

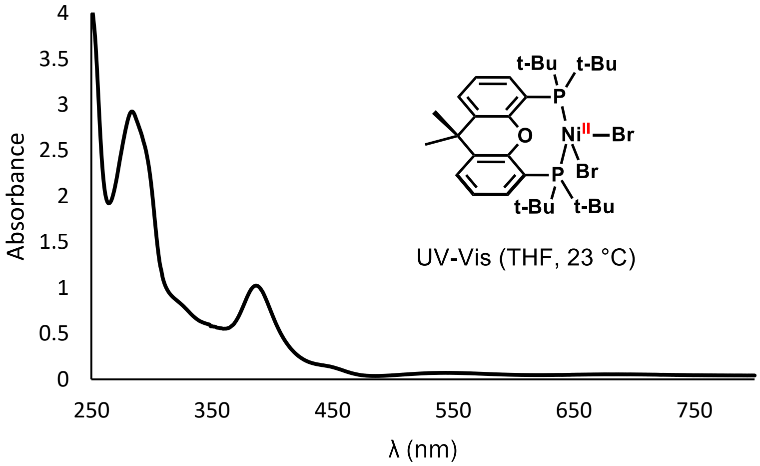

UV-Vis (THF, 23 °C)

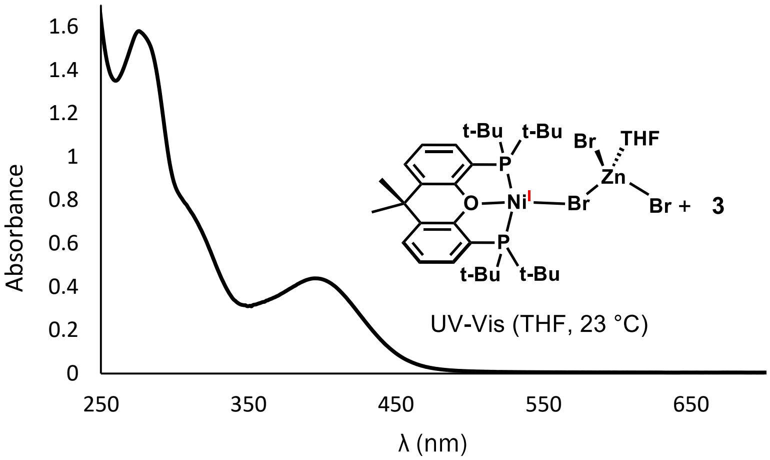

UV-Vis (THF, 23 °C)

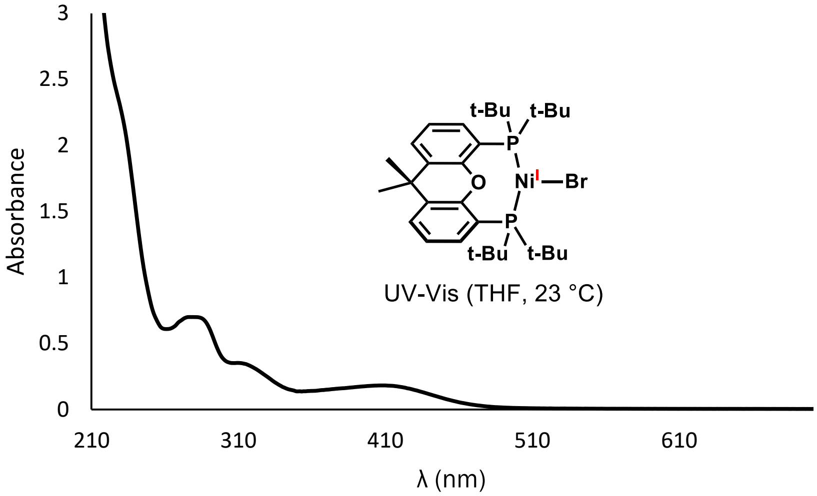
Absorbance
3
2.5
2
1.5
1
0.5
0
210
310
410
510
610
λ (nm)
t-Bu
t-Bu
P
O
Ni^I
Br
P
t-Bu
t-Bu
UV-Vis (THF, 23 °C)

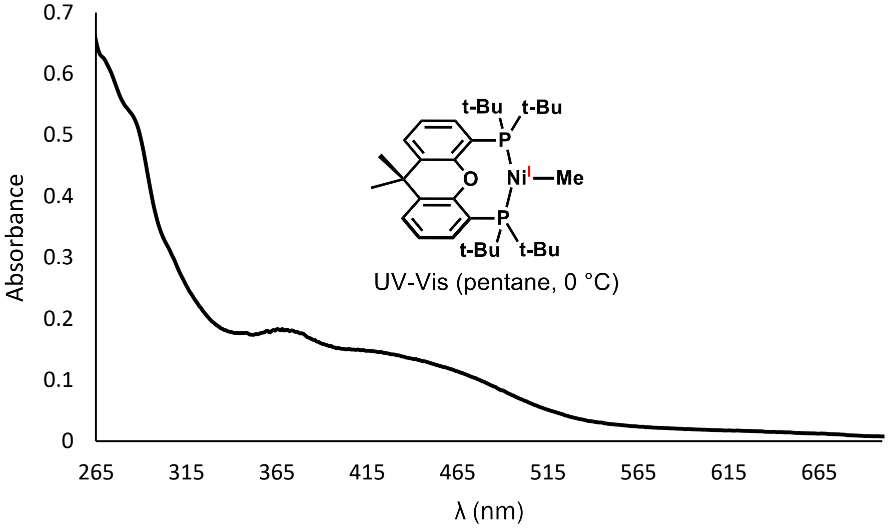
Absorbance
0.7
0.6
0.5
0.4
0.3
0.2
0.1
0
265
315
365
415
465
515
565
615
665
λ (nm)
t-Bu
t-Bu
P
O
Ni^I
Me
P
t-Bu
t-Bu
UV-Vis (pentane, 0 °C)

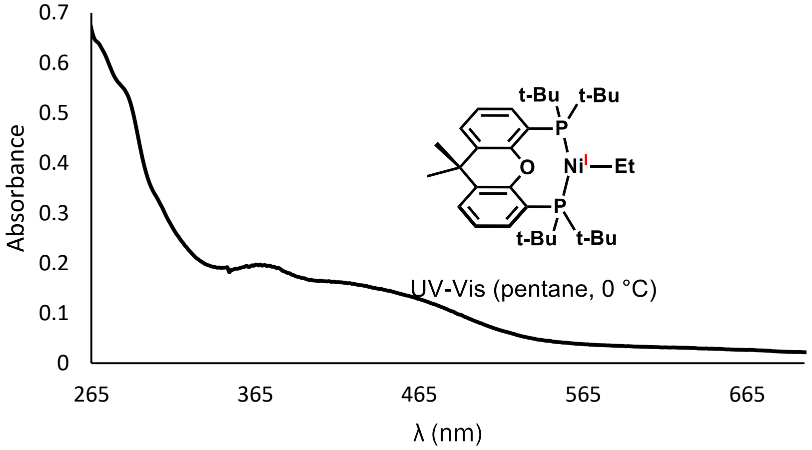
Absorbance
0.7
0.6
0.5
0.4
0.3
0.2
0.1
0
265
365
465
565
665
λ (nm)
t-Bu
t-Bu
P
O
Ni^I
Et
P
t-Bu
t-Bu
UV-Vis (pentane, 0 °C)

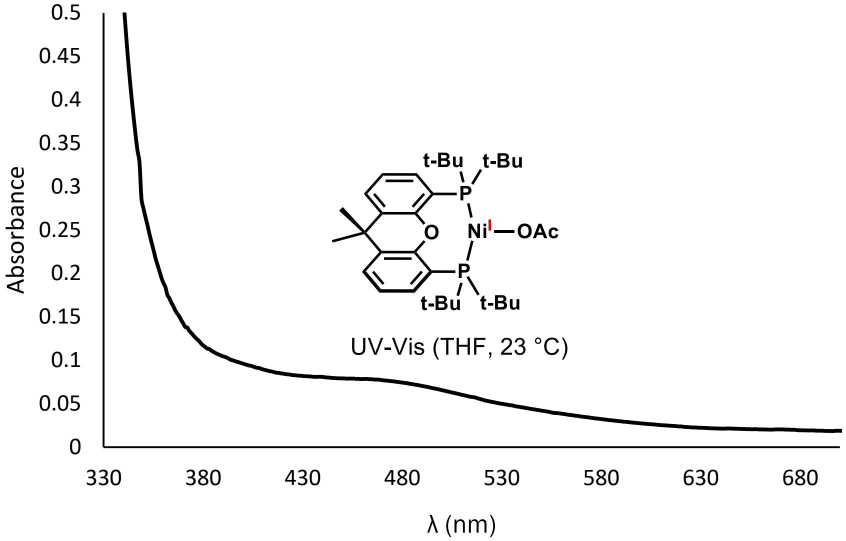
0.5
0.45
0.4
0.35
0.3
0.25
0.2
0.15
0.1
0.05
0
Absorbance
330
380
430
480
530
580
630
680
λ (nm)
t-Bu
t-Bu
P
O
Ni^{I}—OAc
P
t-Bu
t-Bu
UV-Vis (THF, 23 °C)

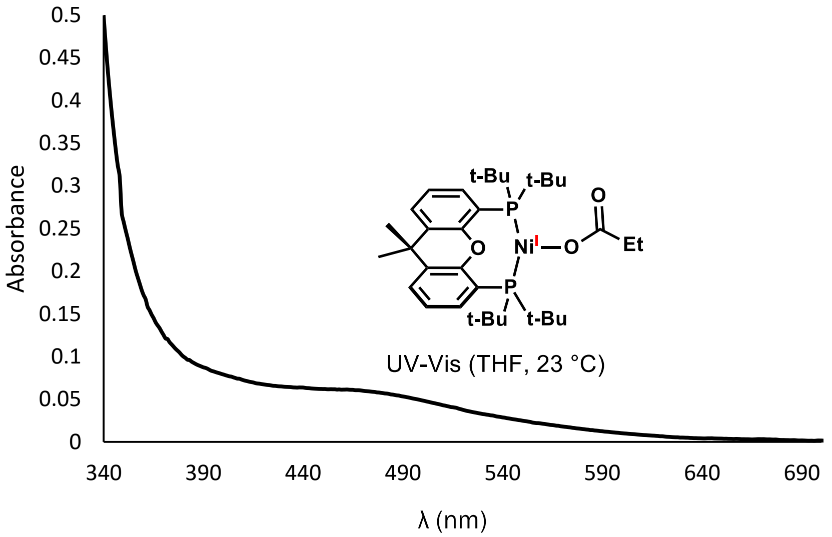
0.5
0.45
0.4
0.35
0.3
0.25
0.2
0.15
0.1
0.05
0
Absorbance
340
390
440
490
540
590
640
690
λ (nm)
t-Bu
t-Bu
P
O
Ni^{I}—O
O
Et
P
t-Bu
t-Bu
UV-Vis (THF, 23 °C)

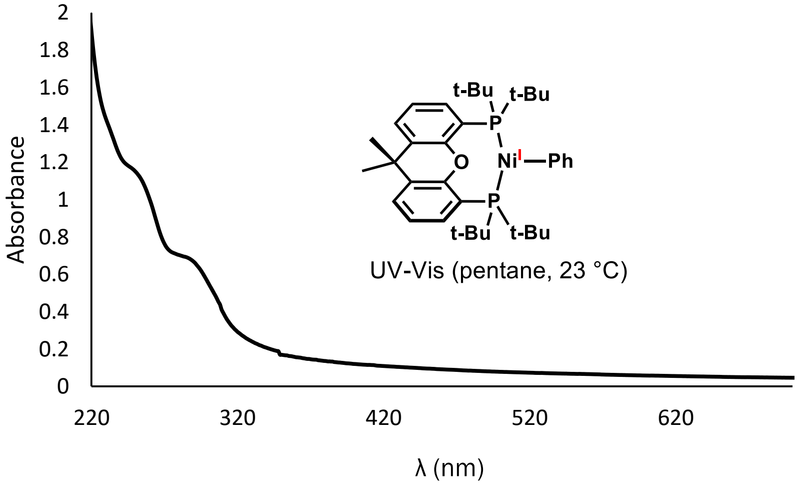
2
1.8
1.6
1.4
1.2
1
0.8
0.6
0.4
0.2
0
Absorbance
220
320
420
520
620
λ (nm)
t-Bu
t-Bu
P
O
Ni^{I}—Ph
P
t-Bu
t-Bu
UV-Vis (pentane, 23 °C)

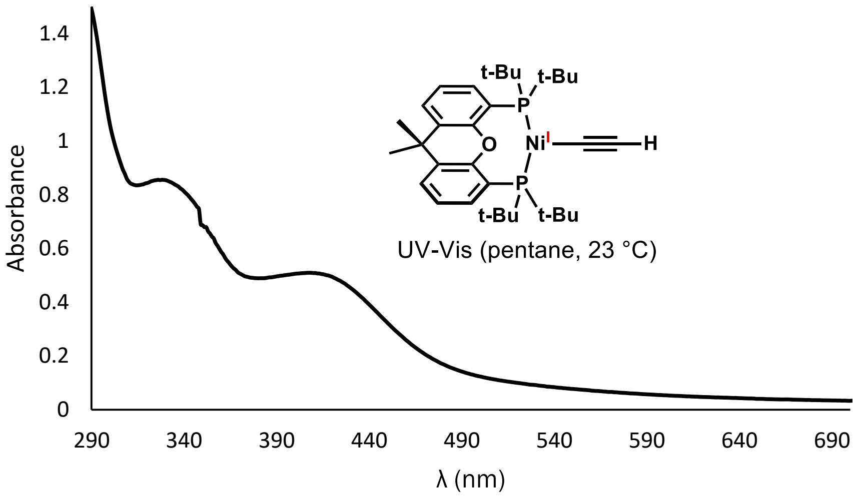
Absorbance
1.4
1.2
1
0.8
0.6
0.4
0.2
0
290
340
390
440
490
540
590
640
690
λ (nm)
t-Bu
t-Bu
P
O
Ni^I
H
P
t-Bu
t-Bu
UV-Vis (pentane, 23 °C)

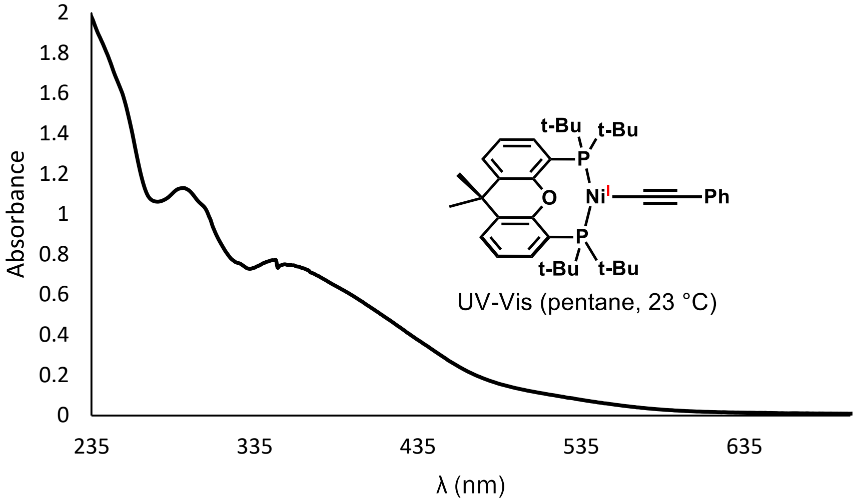
Absorbance
2
1.8
1.6
1.4
1.2
1
0.8
0.6
0.4
0.2
0
235
335
435
535
635
λ (nm)
t-Bu
t-Bu
P
O
Ni^I
Ph
P
t-Bu
t-Bu
UV-Vis (pentane, 23 °C)

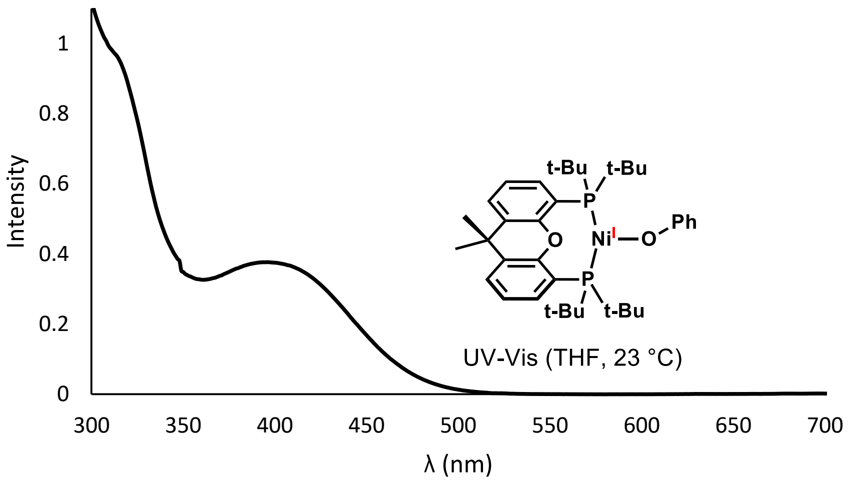
Intensity
1
0.8
0.6
0.4
0.2
0
300
350
400
450
500
550
600
650
700
λ (nm)
t-Bu
t-Bu
P
O
Ni^I
O
Ph
P
t-Bu
t-Bu
UV-Vis (THF, 23 °C)

5. DFT Calculations

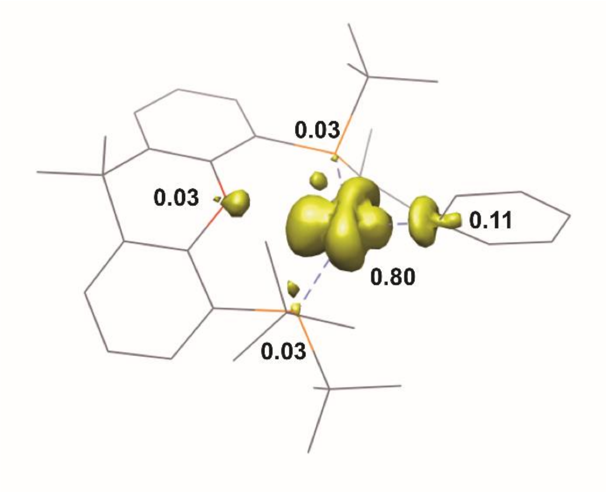

Figure S23. Spin density plot of **11**.

Input File for Energy and Mulliken Spin Density Calculation of (*t*-BuXantphos)Ni(I) Compounds

```
! UKS B3LYP RIJCOSX SlowConv TightSCF def2-SV(P) def2-SVP/J Normalprint UCO OPT
%basis NewGTO 28 "def2-TZVP(-f)" end
NewGTO 8 "def2-TZVP(-f)" end
NewGTO 15 "def2-TZVP(-f)" end
NewAuxGTO 28 "def2-TZVP/J" end
NewAuxGTO 8 "def2-TZVP/J" end
NewAuxGTO 15 "def2-TZVP/J" end
end

%scf
MaxIter 1000
TolE 1E-7
TolErr 1E-6
```

```
end

* xyz 0 2
xyz coordinates from X-ray structures
*

%plots format cube
dim1 100 dim2 100 dim3 100
SpinDens("name.cube");
end
```

6. EPR Spectra

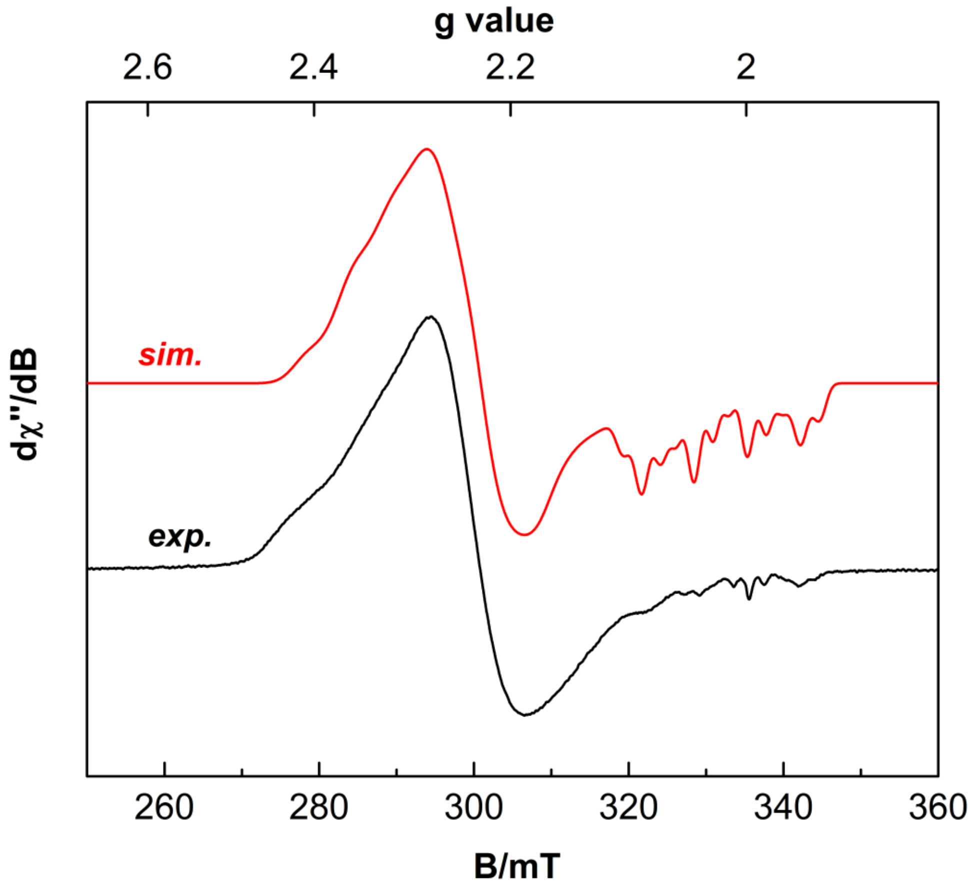

Figure S24. X-band EPR spectrum of Ni(I)Br **3** recorded in toluene glass at 10 K. Spectroscopic parameters for **3**: $g_x = 2.32$, $g_y = 2.23$, $g_z = 2.02$, $A_{1,1} = 189$ MHz, $A_{1,2} = 134$ MHz, $A_{1,3} = 60$ MHz, $A_{2,1} = 177$ MHz, $A_{2,2} = 70$ MHz, $A_{2,3} = 75$ MHz, $A_{3,1} = 107$ MHz, $A_{3,2} = 66$ MHz, $A_{3,3} = 186$ MHz.

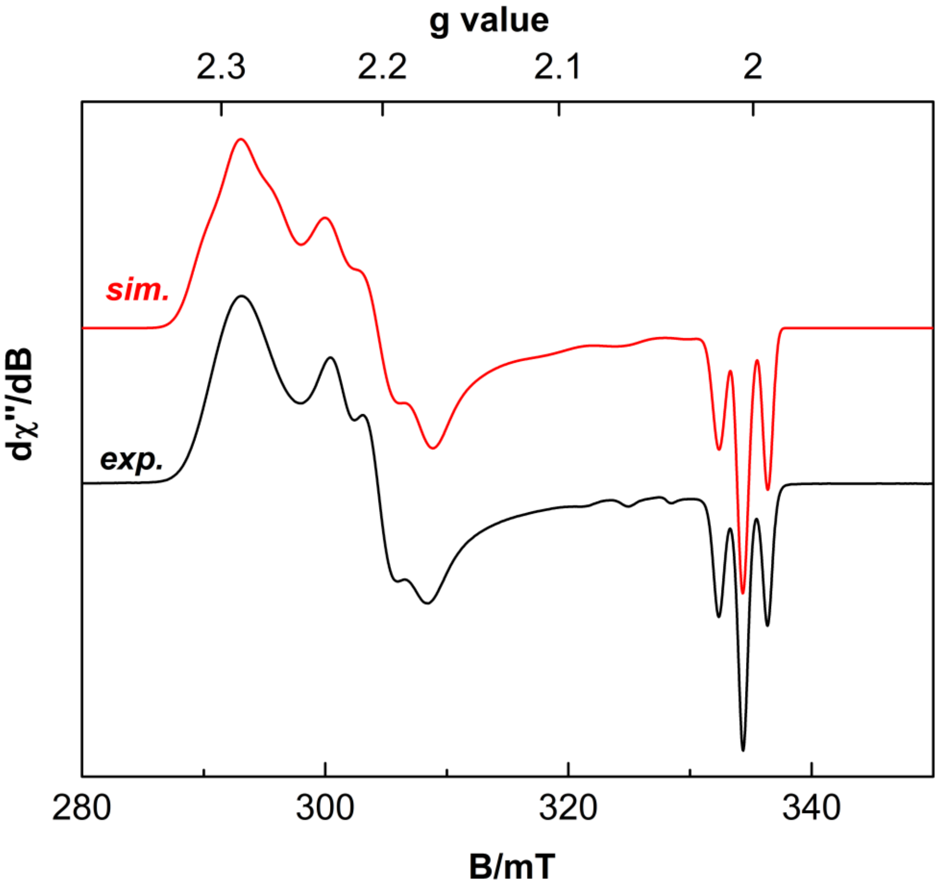

Figure S25. X-band EPR spectrum of Ni(I)Me **4** recorded in toluene/Et_2O at 10 K. Spectroscopic parameters for **4**: $g_x = 2.29$, $g_y = 2.20$, $g_z = 2.00$, $A_{1,1} = 96$ MHz, $A_{1,2} = 80$ MHz, $A_{1,3} = 52$ MHz, $A_{2,1} = 77$ MHz, $A_{2,2} = 117$ MHz, $A_{2,3} = 60$ MHz.

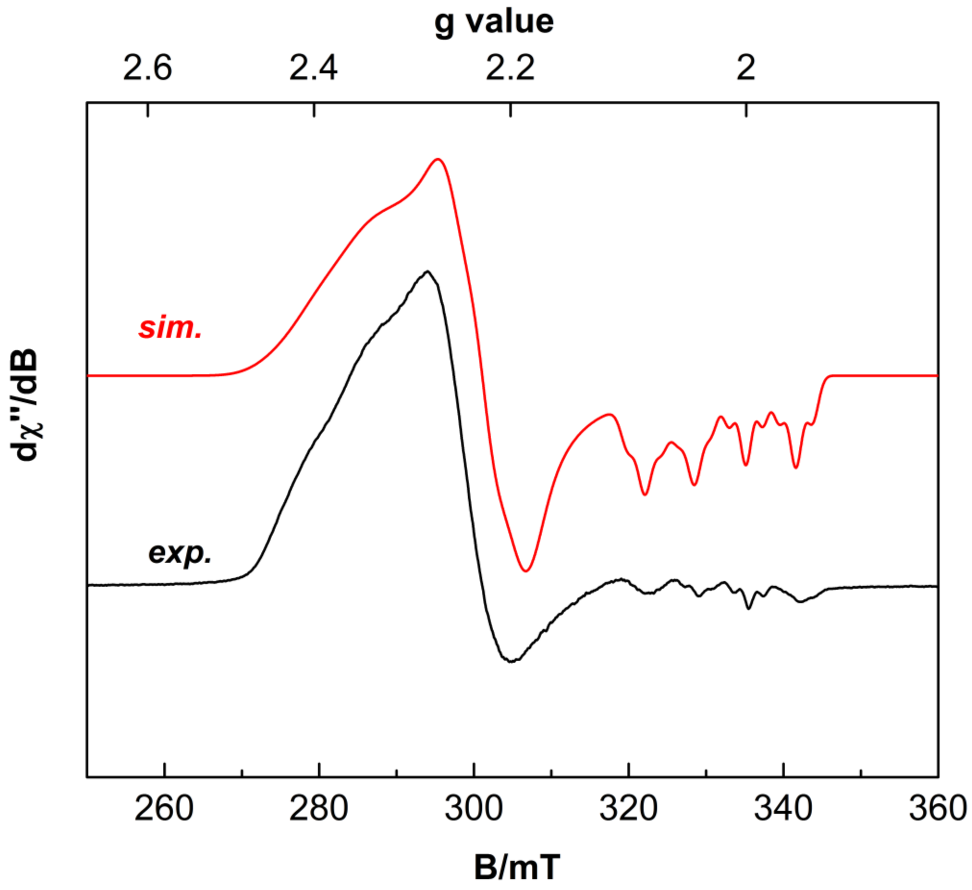

Figure S26. X-band EPR spectrum of Ni(I)OAc **9** recorded in toluene/Et_2O at 10 K. Spectroscopic parameters for **9**: g_x = 2.34, g_y = 2.22, g_z = 2.02, $A_{1,1}$ = 270 MHz, $A_{1,2}$ = 120 MHz, $A_{1,3}$ = 370 MHz, $A_{2,1}$ = 165 MHz, $A_{2,2}$ = 100 MHz, $A_{2,3}$ = 182 MHz, $A_{3,1}$ = 150 MHz, $A_{3,2}$ = 30 MHz, $A_{3,3}$ = 60 MHz, $A_{4,1}$ = 153 MHz, $A_{4,2}$ = 10 MHz, $A_{4,3}$ = 60 MHz.

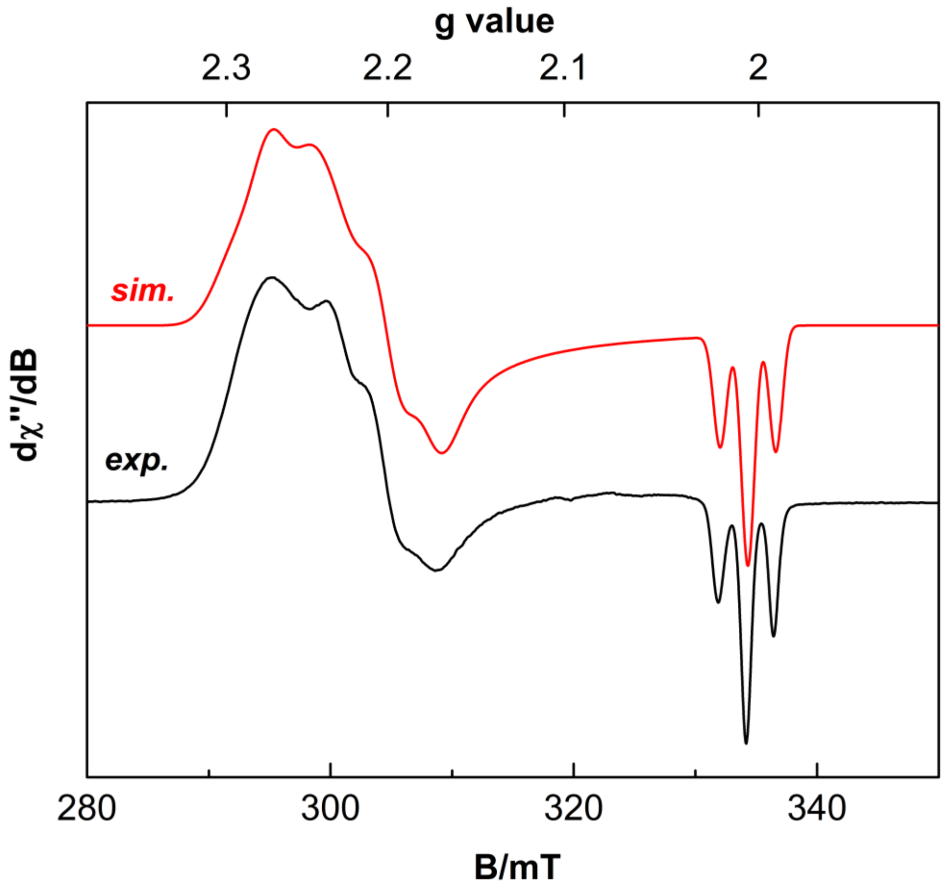

Figure S27. X-band EPR spectrum of Ni(I)Ph **11** recorded in toluene at 10 K. Spectroscopic parameters for **11**: $g_x = 2.27$, $g_y = 2.20$, $g_z = 2.01$, $A_{1,1} = 90$ MHz, $A_{1,2} = 106$ MHz, $A_{1,3} = 62$ MHz, $A_{2,1} = 106$ MHz, $A_{2,2} = 90$ MHz, $A_{2,3} = 66$ MHz.

---

1. Song, S.; Xiao, T.; Wang, L.; Redshaw, C.; Wang, F.; Sun, W.-H. *J. Organometal. Chem.*, **2012**, *699*, 18.
2. The cryoprobe is supported by NIH under grant number S10 OD016343.
3. Stoll, S.; Schweiger, A. J. *Magn. Reson.* **2006**, *178*, 42.
4. Beattie, D. D.; Schareina, T.; Beller, M. *Org. Biomol. Chem.* **2017,** *15* (20), 4291-4294.